Enhanced validation data

Anti-Met (c-Met) recombinant antibody – ab216574

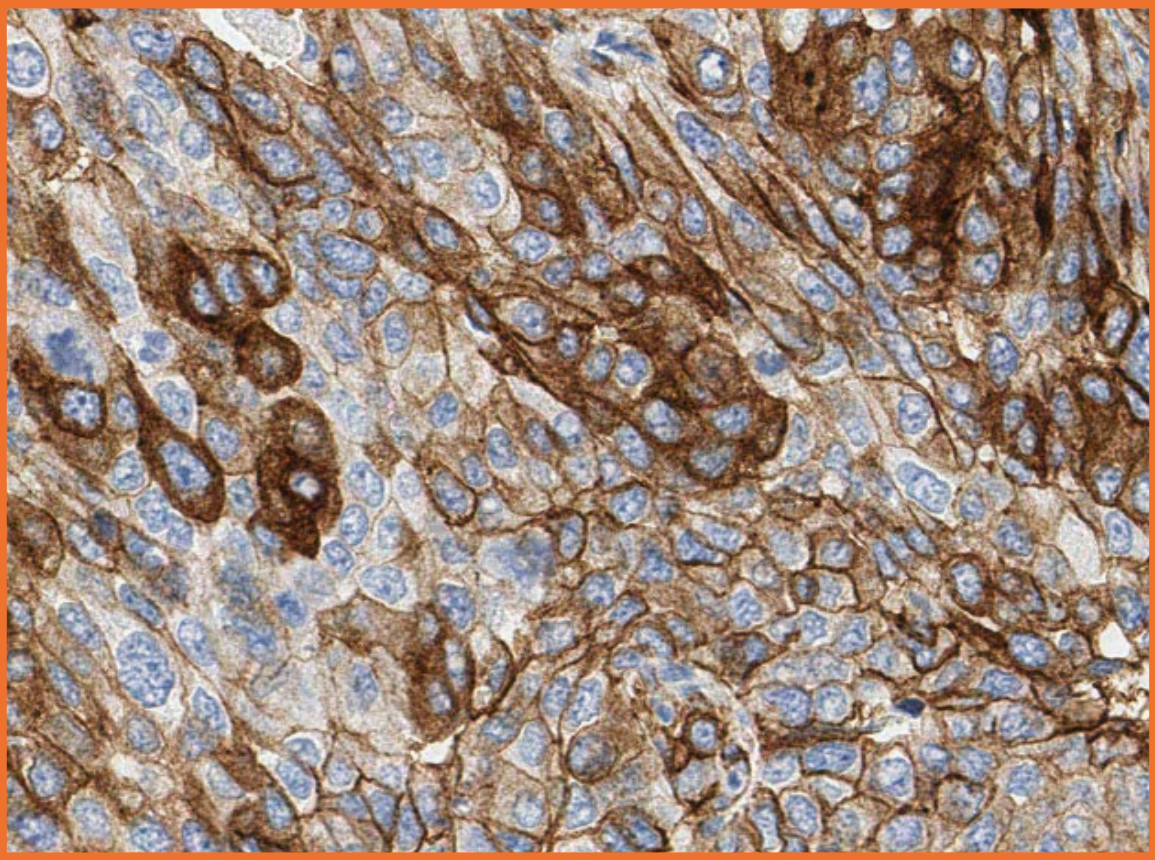

progress happens together

abcam

AB0407_v1.0_121824

Enhanced validation of Anti-Met (c-Met) recombinant antibody [EPR19067] – ab216574

Enhanced validation designed for your needs

We understand the challenge of finding the right antibody clone – highly specific and sensitive to your intended target – at early selection stages of your development program. To de-risk this clone selection process for you, we generated enhanced validation data for our best recombinant antibody clones to some of the most promising targets.

Our enhanced validation gives you an extra level of confidence in an antibody clone

— Provides additional data on the specificity and sensitivity of our recombinant antibodies in immunohistochemistry (IHC) and other relevant techniques

— Carried out in a custom manner, specific both to the target and the relevant research & clinical settings

— Builds upon our high-quality standard validation

Our framework for enhanced validation

— Our enhanced validation focuses on generating detailed IHC expression profiles for promising oncology targets in selected formalin-fixed paraffin-embedded (FFPE) human normal tissues and cancer tissue microarrays (TMAs).

— In this study, we demonstrate the sensitivity and specificity of Anti-Met (c-Met) antibody (ab216574) in IHC in selected tissues and TMAs using a BOND™ RX Research Stainer (Leica®) and DISCOVERY ULTRA system (Roche Diagnostics).

— A quantitative H-score analysis of c-Met expression was performed using the artificial intelligence (AI)-driven digital image analysis software Visiopharm® (Visiopharm A/S).

AB0407_v1.0_121824

Target overview

HGNC symbol
MET

Approved name
MET (mesenchymal–epithelial transition factor) proto-oncogene, receptor tyrosine kinase)

Chromosomal location
7q31.2

Function

- The hepatocyte growth factor (HGF) /c-MET signaling pathway is essential in many cellular processes in various cancer cells, including carcinogenesis, proliferation [1-6], survival [7,8], metastasis [9-12], tumor microenvironment regulation [13], metabolic reprogramming [14], epithelial-mesenchymal transition [15-17], stemness [18-23], and drug resistance [24-29].

Tissue specificity

- c-MET is typically expressed by epithelial cells and is often overexpressed and amplified in various human tumors [30-34].

Cellular localization

- Cell membrane; also secreted.

Database links

Entrez Gene: 4233
OMIM®: 164860
Uniprot: P08581

Materials and methods

Human tissues were selected based on the target's expression and its current relevance to ongoing research and clinical trials. Gene expression was further analyzed for oncology targets in cBioPortal for Cancer Genomics using the Cancer Genome Atlas (TCGA) PanCancer Atlas datasets [35-38].

Tissue microarray (TMA)	Cores	Cases	Normal/ Benign cases	Cancer cases	Source (#catalog number)
Multi-normal [(a)]	15	15	15	0	In-house TMA
Multi-cancer [(b)]	40	35	1	34	In-house TMA
Cervix cancer	102	102	5	97	Pantomics (#CXC1021)
Lung cancer	102	102	5	97	Pantomics (#COC1021)
Breast cancer	96	48	0	48	Pantomics (#BRC964)

Table 1. List of human TMAs used in the enhanced validation. All tissues were sourced from Abcam-approved tissue suppliers.

a) The multinormal TMA consists of the following tissues from one donors: colon, cerebrum, tonsil, stomach, testis, prostate, lung, skeletal muscle, heart, skin, spleen, pancreas, kidney, placenta and liver.

b) The multicancer TMA consists of the following tissues from two donors: seminoma, prostate adenocarcinoma, bladder carcinoma, renal cell carcinoma, melanoma, stomach adenocarcinoma, pancreatic adenocarcinoma, hepatocellular carcinoma, ovaria carcinoma, cervical cancer, head and neck carcinoma and endometrial cancer. The following tissues were from single donors: lung (squamous cell carcinoma (SCLC) and non-squamous cell carcinoma (NSCLC)), colon (adenocarcinoma and invasive adenocarcinoma), breast (ductal carcinoma and invasive lobular carcinoma), B-cell lymphoma, T-cell lymphoma, gliomas (grade II and IV) and placenta.

Step	Reagents	Method
Deparaffinization	DISCOVERY Wash (RUO)	Standard
Cell conditioning	ULTRA Cell Conditioning Solution (ULTRA CC2)	64 min, 100 °C
Pre-primary peroxidase inhibitor	OptiView Peroxidase Inhibitor	4 min
Primary antibody	Anti-C-MET antibody [EPR19067] – ab216574 diluted in Bond™ primary antibody diluent (#AR9352) to final concentration of 0.05 µg/mL	16 min, 37 °C
Counterstain	Hematoxylin II	8 min
Post counterstain	Bluing Reagent	4 min

Table 2 . IHC staining protocol on the DISCOVERY ULTRA (Roche Diagnostics) instrument. Staining was performed using standard conditions with OptiView DAB IHC Detection kit (#760-700).

Enhanced validation data

Step	Reagents	Method
Dewax	Bond™ dewax solution (AR922), alcohol, BOND wash solution (AR9590)	Dewax
Antigen retrieval	Bond™ epitope retrieval ER2 solution (AR9640)	HIER with ER2 (pH 9.0), 20 min, 100°C

Step	Reagents	Number of washes	Time (minutes)
Peroxide block	3-4% (v/v) Hydrogen peroxide	-	5
Wash	Bond™ wash solution	3x	0
Primary antibody	Anti-C-MET antibody [EPR19067] – ab216574 diluted in Bond™ primary antibody diluent (#AR9352) to final concentration of 0.05 µg/mL	-	15
Wash	Bond™ wash solution	4x	0
Secondary antibody	Bond™ polymer refine detection (DS9800)	-	8
Wash	Bond™ wash solution	2x	4
	Deionized water	1x	0
Visualization	Mixed DAB refine (DS9800)	1x	0
	Mixed DAB refine (DS9800)	-	10
Wash	Deionized water	3x	0
Counterstain	Hematoxylin (DS9800)	-	5
Wash	Deionized water	1x	0
	Bond™ wash solution	1x	0
	Deionized water	1x	0

Table 3. IHC staining protocol on BOND™ RX Research Stainer (Leica®). The protocol used is the same as the default IHC protocol F on BOND™ RX Research Stainer (Leica®), apart from the standard post-primary step, which has been excluded from our protocol. All steps were performed at room temperature.

H-score analysis

A quantitative H-score analysis of c-MET expression was performed using the artificial intelligence (AI)- driven digital image analysis software Visiopharm® (Version: 2023.09). TMA slides were de-arrayed and the tissue within each core was detected. Tissue detection and artefact exclusion were performed using models with DeepLabv3+ architecture.

Total cell numbers for each core were counted using a trained AI model with U-Net architecture. Using the cell analysis data and thresholds, H-scores of the whole core in the TMAs were calculated in Visiopharm® and the graphical representation was generated using GraphPad Prism 10.

Raw IHC image | Cell detection

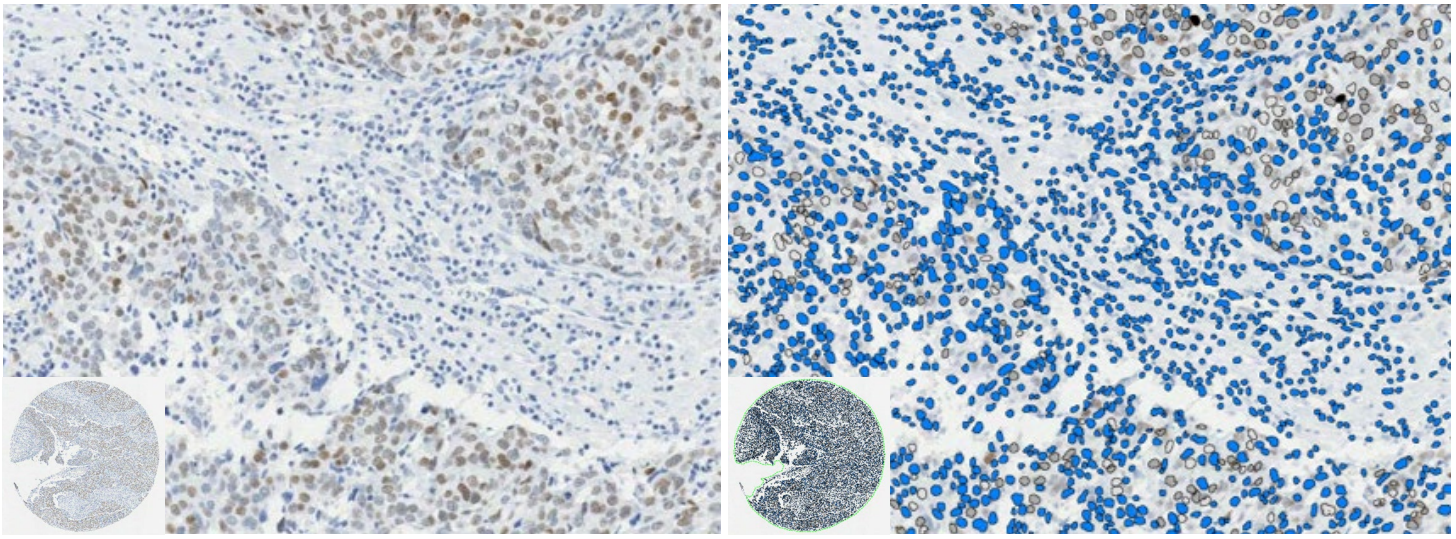

Figure 1. Raw IHC images were subjected to total cell detection to determine staining intensity. There are four intensity scores shown here: blue (0), white (1+), grey (2+) and black (3+).

IHC staining	Corresponding intensity score	Visiopharm® intensity threshold
Negative	0	> 295
Weak	1+	< 295
Moderate	2+	< 160
Strong	3+	< 80

Table 4. Intensity scoring and thresholds for H-score analysis. The H-score captures both the IHC staining intensity and the percentage of stained cells at each intensity level. It was calculated using the formula H-score = [(0x % of negative cells) + (1x % of weak stained cells) + (2x % of moderate stained cells) + (3x % of strong stained cells), giving an analytical range from 0 to 300.

c-MET expression in multi-normal TMA (BOND™ RX)

Below are the representative images of selected tissues from multi-normal TMA. c-MET expression was detected in the brain, stomach, breast, lung, tonsil, spleen, prostate, lymph node and kidney.

c-Met

Brain (Cerebrum)

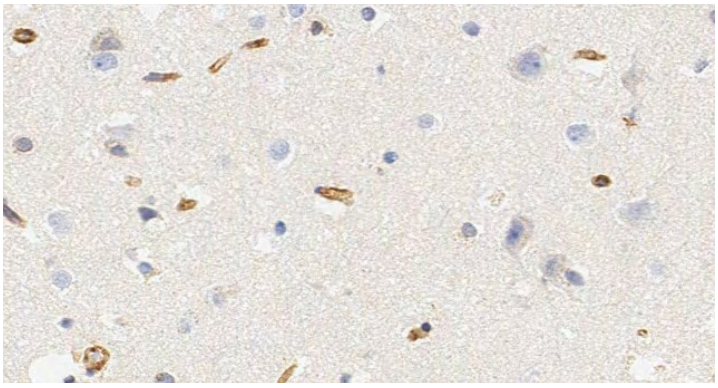

Stomach

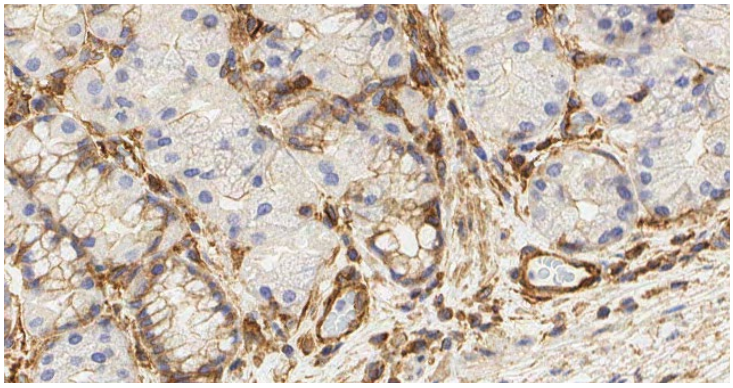

Breast

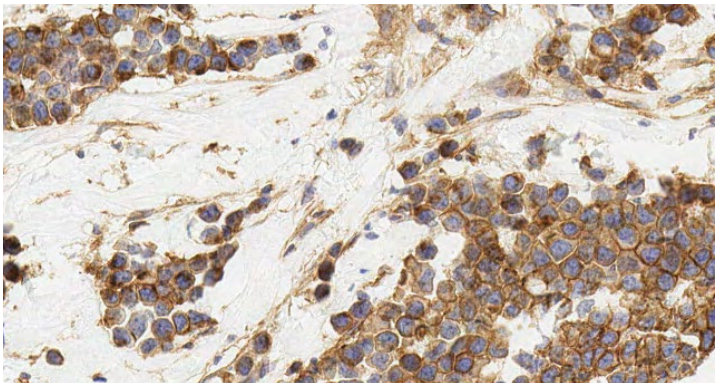

Lung

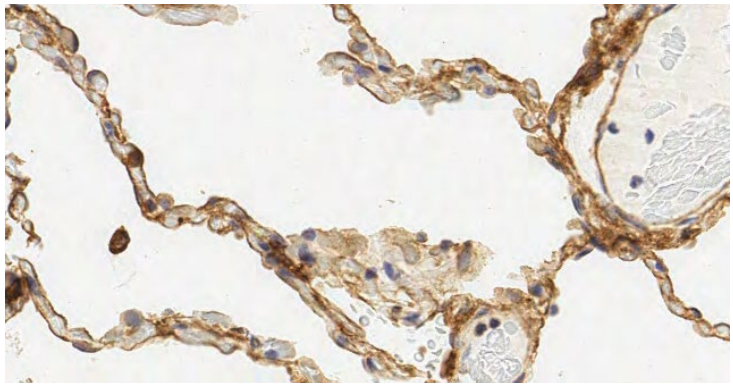

Tonsil

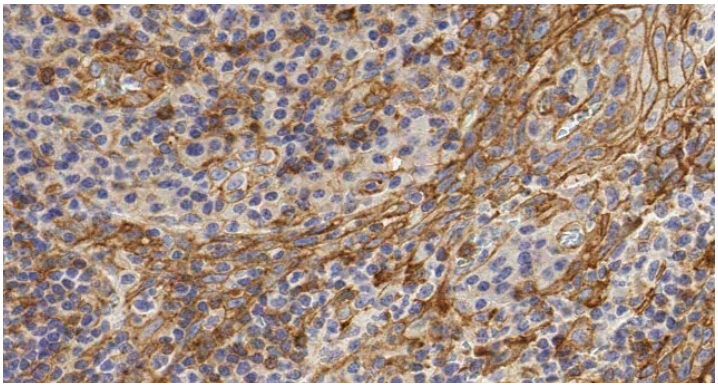

Spleen

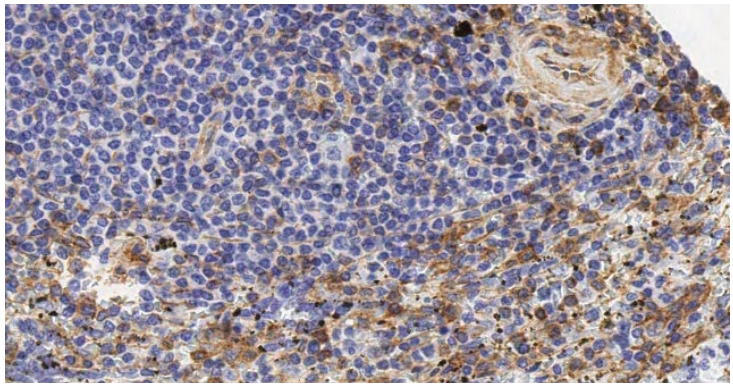

c-Met

Prostate	Lymph node
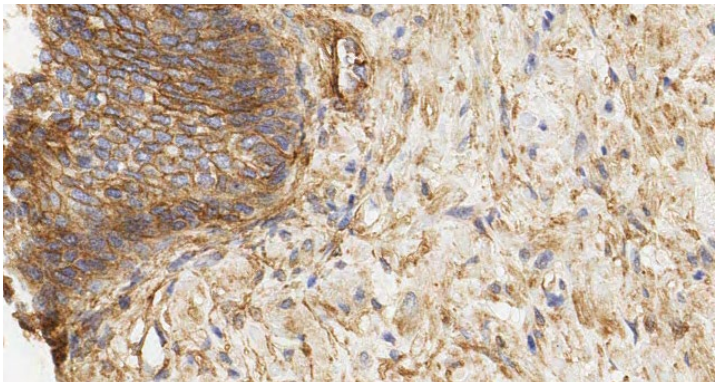	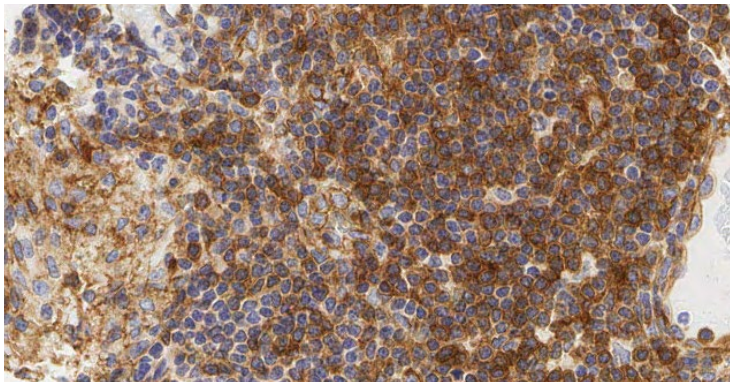
Kidney	**Isotype control - Kidney**
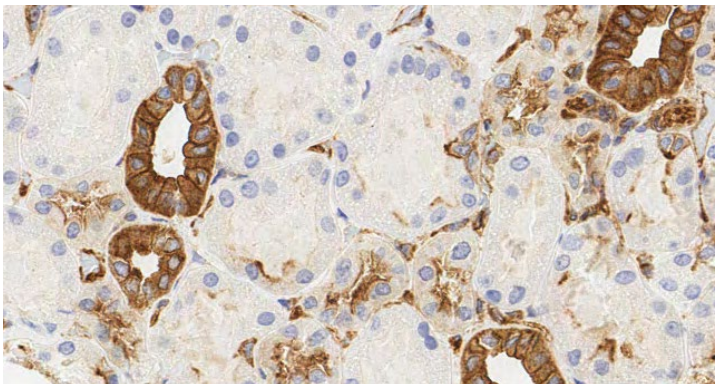	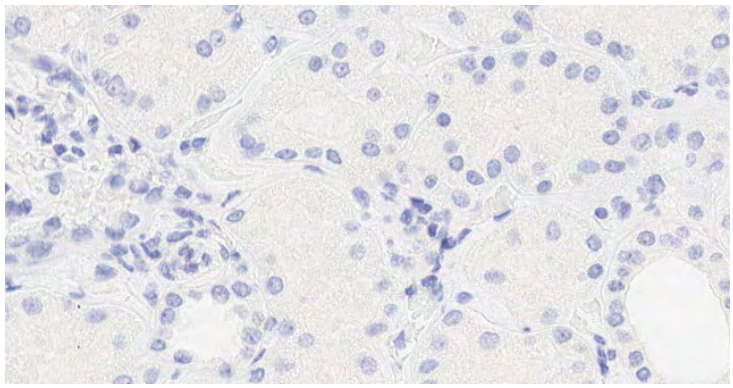

Figure 2. c-MET expression in human normal tissue. IHC staining of multi-normal human tissues using anti-c-Met (ab216574) or anti-rabbit IgG-isotype control antibody (0.5 µg/mL) (ab172730). Positive staining in brown; nuclear hematoxylin counterstain in blue. Slides were scanned at 20x on Aperio® AT2 and imaged at 20x on Aperio® ImageScope.

c-MET expression in multi-cancer TMA (BOND™ RX)

Below are the representative images of selected tissues from multi-cancer TMA. c-MET expression was detected in breast cancer (ductal and invasive lobular carcinoma), ovarian carcinoma, endometrial cancer, non-small cell lung carcinoma, renal cell carcinoma, bladder carcinoma, seminoma, head and neck cancer, T-cell lymphoma and invasive colon adenocarcinoma.

c-Met

Breast ductal carcinoma

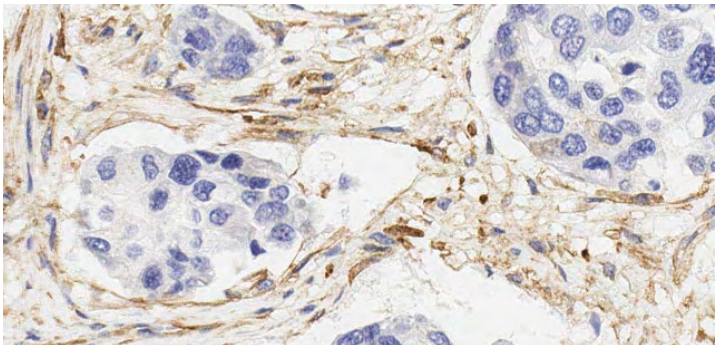

Breast-invasive lobular carcinoma

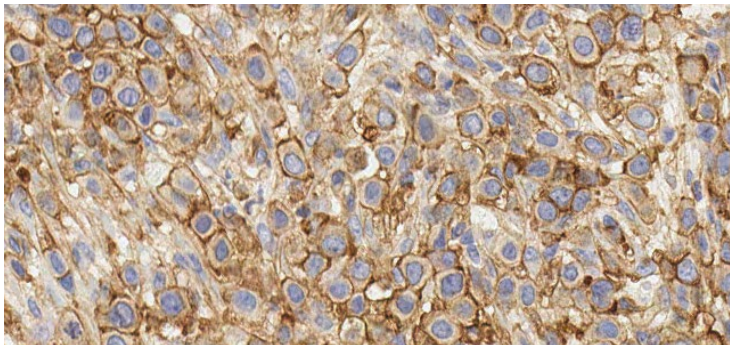

Ovarian carcinoma

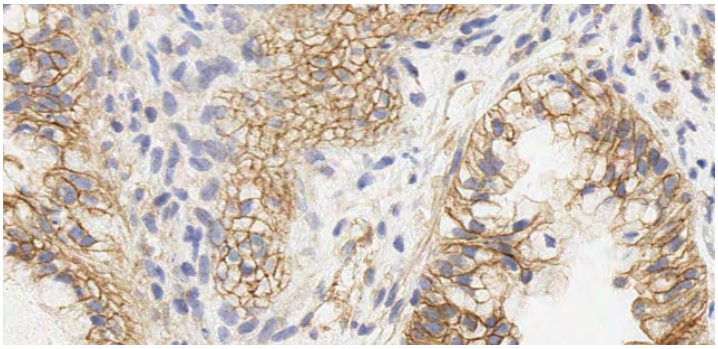

Endometrial cancer

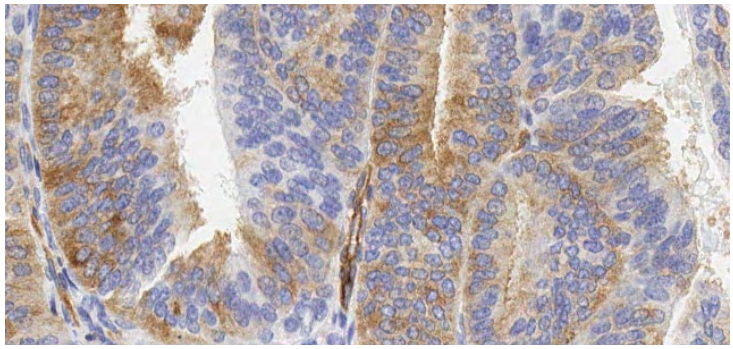

Non-small cell lung carcinoma

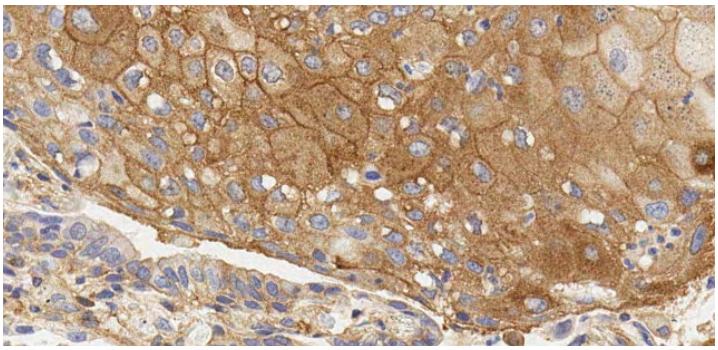

Renal cell carcinoma

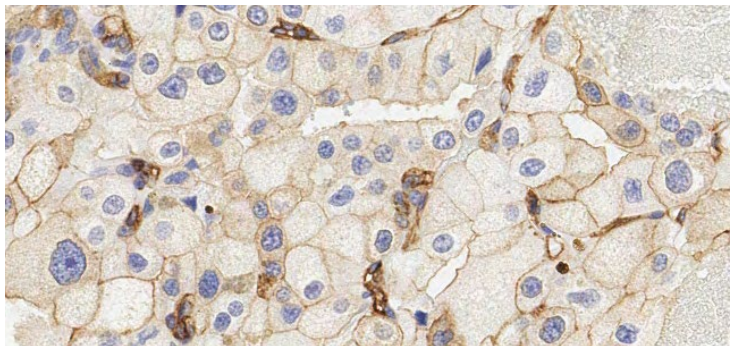

c-Met

Bladder carcinoma

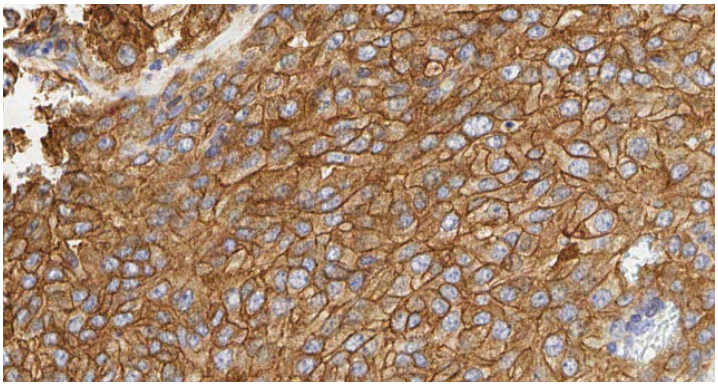

Seminoma

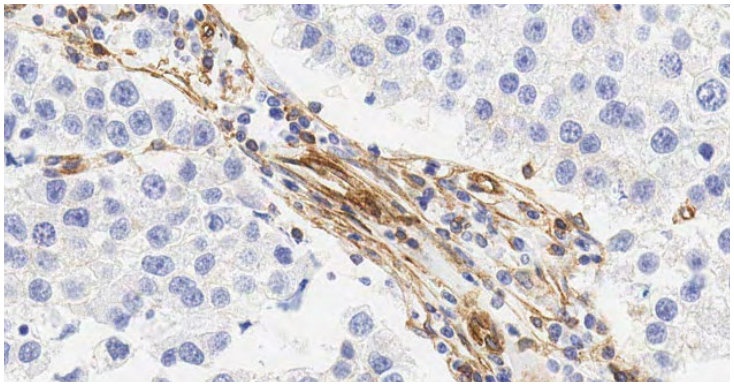

Head & neck cancer

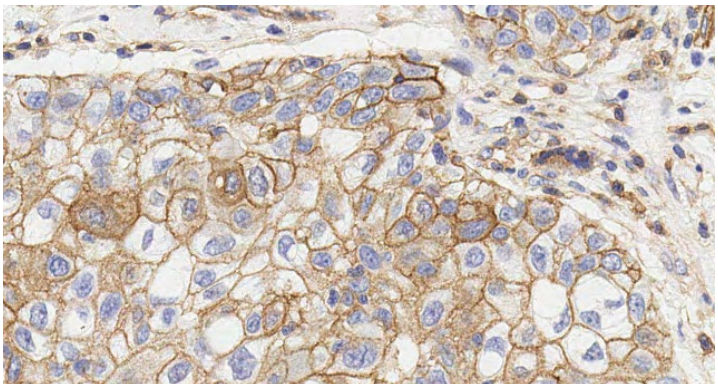

T cell lymphoma

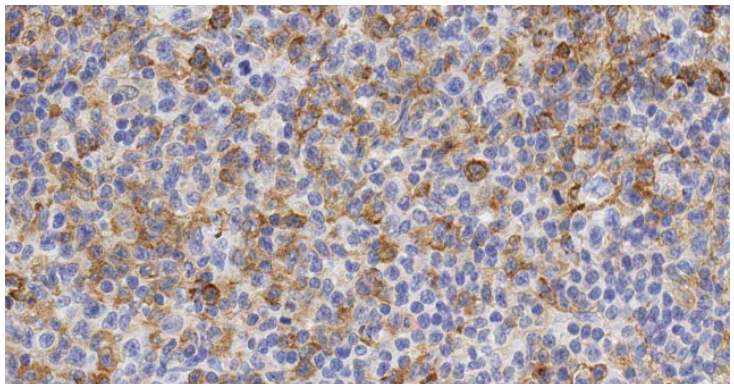

Invasive colon adenocarcinoma

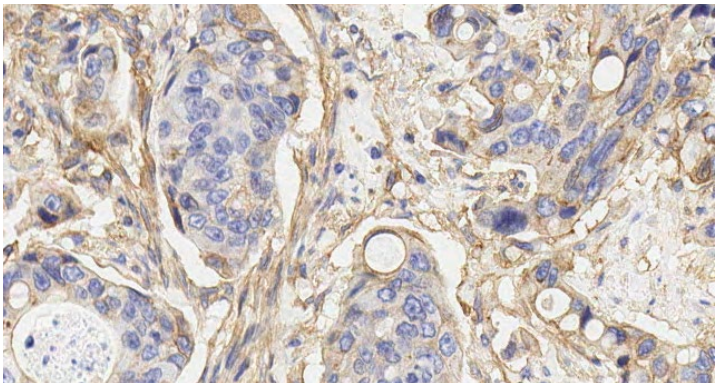

Invasive colon adenocarcinoma - Isotype control

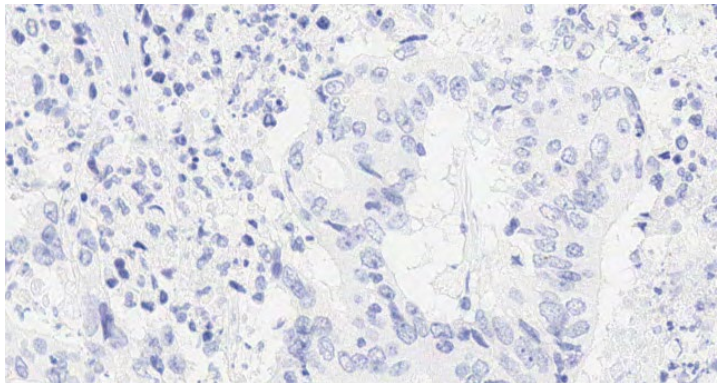

Figure 3. c-MET expression in cancer. IHC staining of multi-cancer human tissues using anti- c-Met (ab216574) or anti-rabbit IgG-isotype control antibody (0.5 µg/mL) (ab172730). Positive staining in brown; nuclear hematoxylin counterstain in blue. Slides were scanned at 20x on Aperio® AT2 and imaged at 20x on Aperio® ImageScope.

c-MET expression in multi-normal TMA (DISCOVERY ULTRA)

Below are the representative images of selected tissues from multi-normal TMA. Below are the representative images of selected tissues from multi-normal TMA. c-MET expression was detected in the brain, pancreas, colon, lung, tonsil, spleen, breast, lung, tonsil, spleen, prostate, testis and placenta.

c-Met

Brain (Cerebrum)

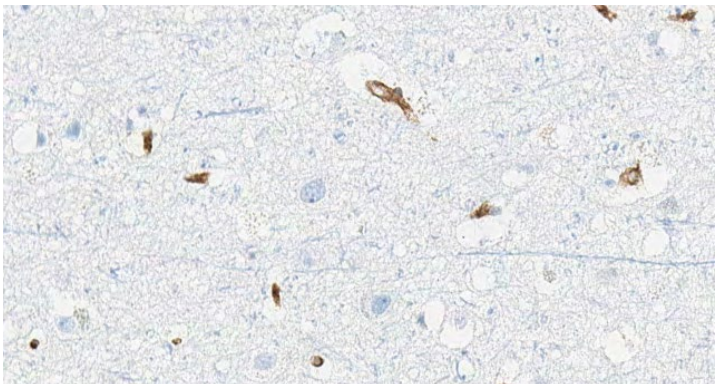

Pancreas

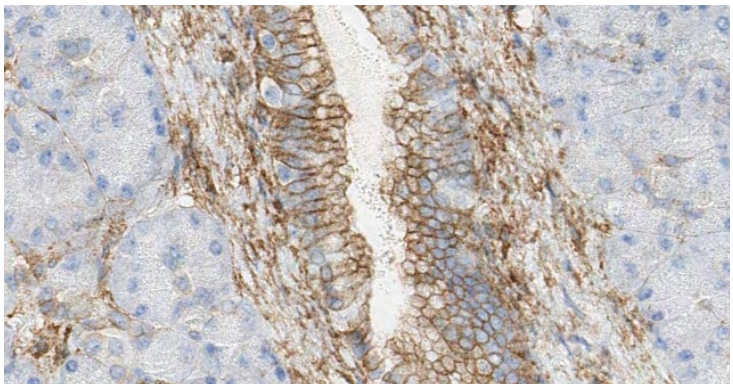

Colon

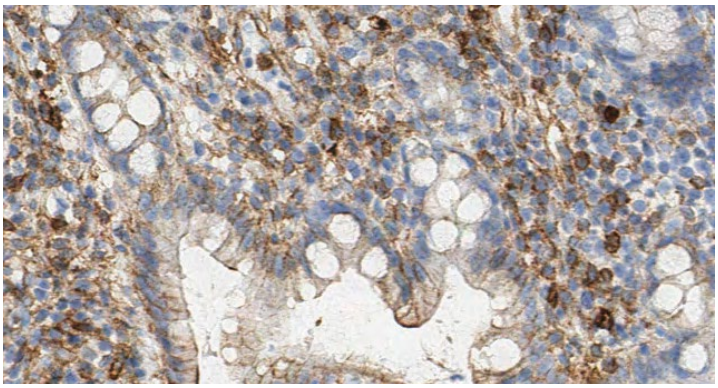

Lung

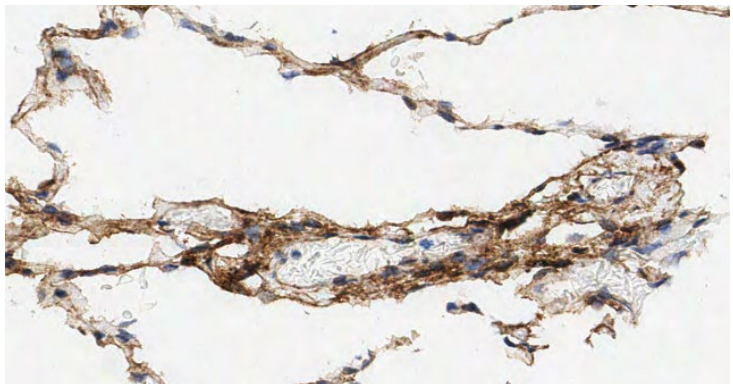

Tonsil

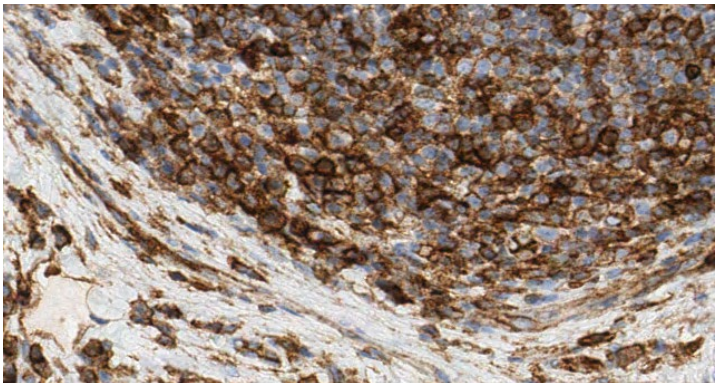

Spleen

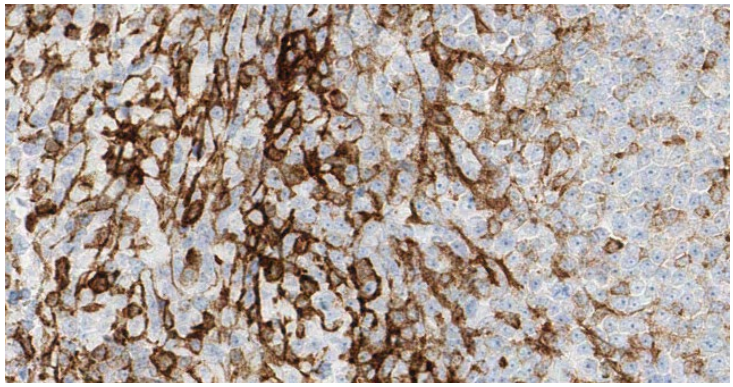

c-Met

Prostate	Testis
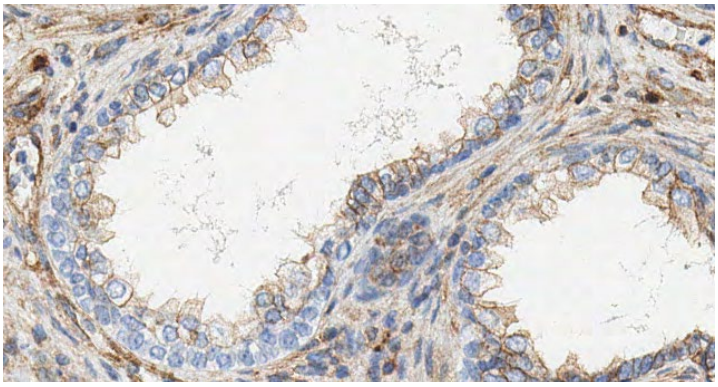	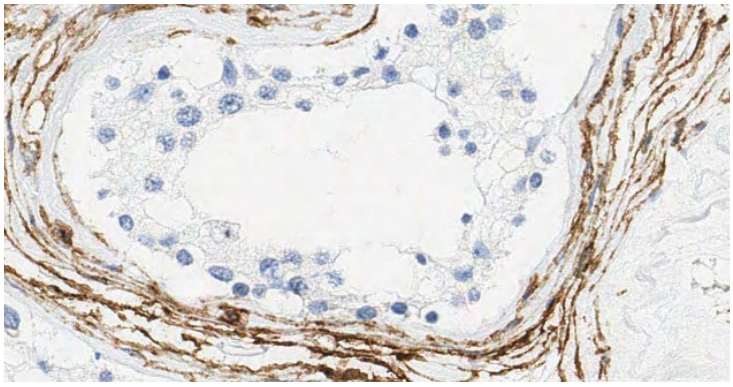
Placenta	**Isotype control**
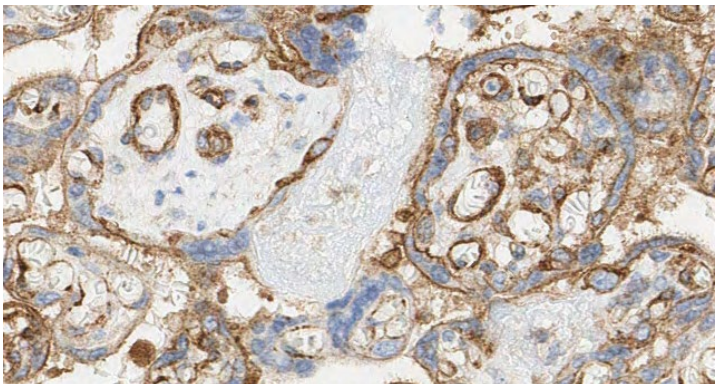	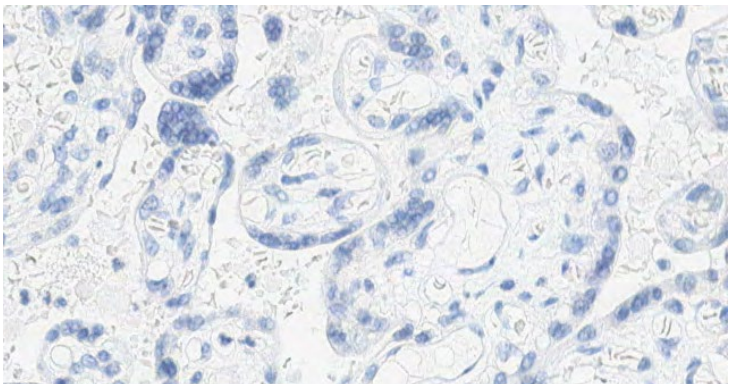

Figure 4. c-MET expression in human normal tissue. IHC staining of multi-normal human tissues using anti- c-Met (ab216574) or anti-rabbit IgG-isotype control antibody (ab172730). Positive staining in brown; nuclear hematoxylin counterstain in blue. Slides were scanned at 20x on Aperio® AT2 and imaged at 20x on Aperio® ImageScope.

c-MET expression in multi-cancer TMA (DISCOVERY ULTRA)

Below are the representative images of selected tissues from multi-cancer TMA. c-MET expression was detected in breast cancer (ductal and invasive lobular carcinoma), ovarian carcinoma, endometrial cancer, non-small cell lung carcinoma, renal cell carcinoma, bladder carcinoma, seminoma, head and neck cancer, T-cell lymphoma and invasive colon adenocarcinoma.

c-Met

Breast ductal carcinoma

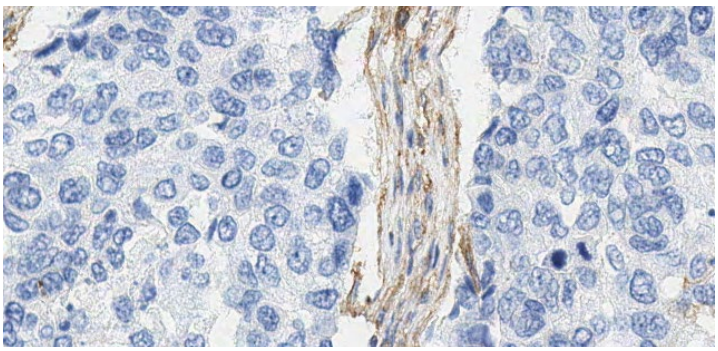

Breast-invasive lobular carcinoma

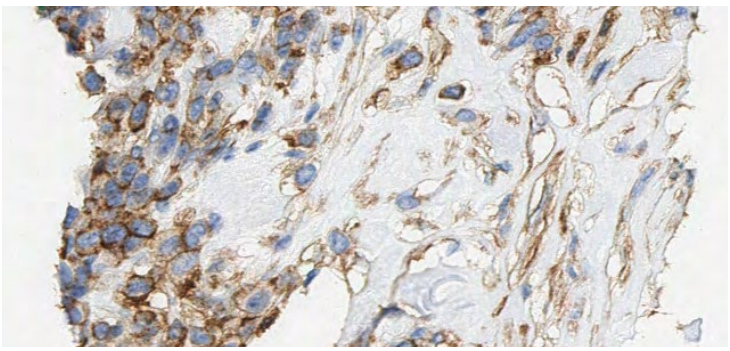

Ovarian carcinoma

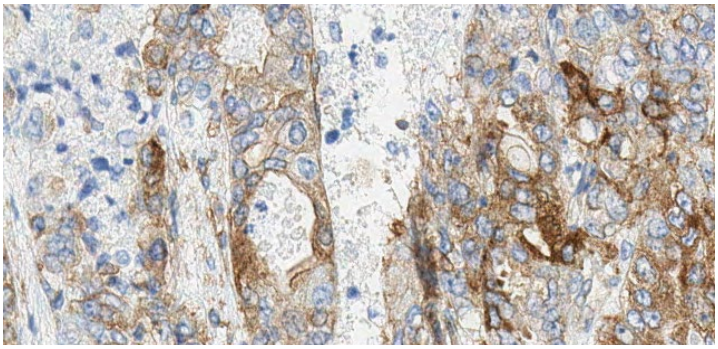

Endometrial cancer

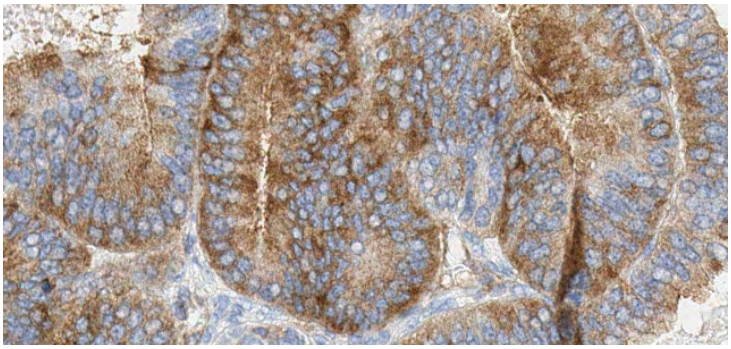

Non-small cell lung carcinoma

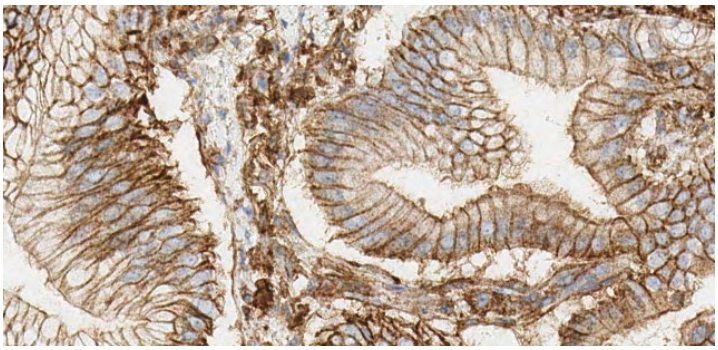

Renal cell carcinoma

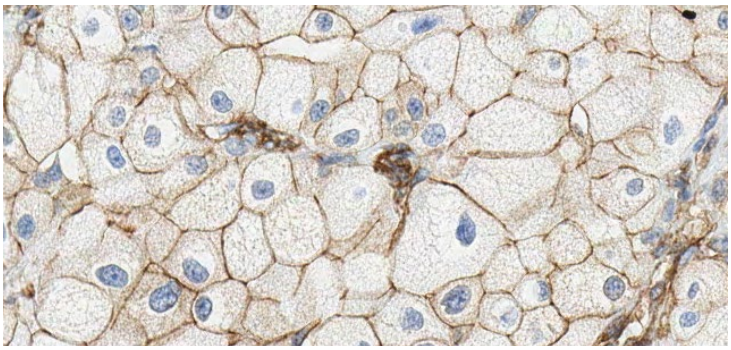

c-Met

Bladder carcinoma

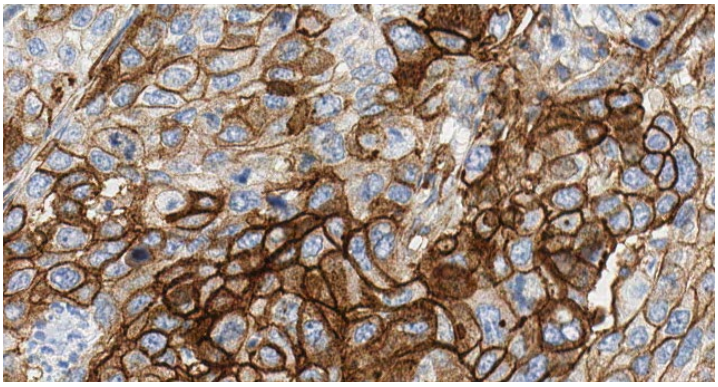

Seminoma

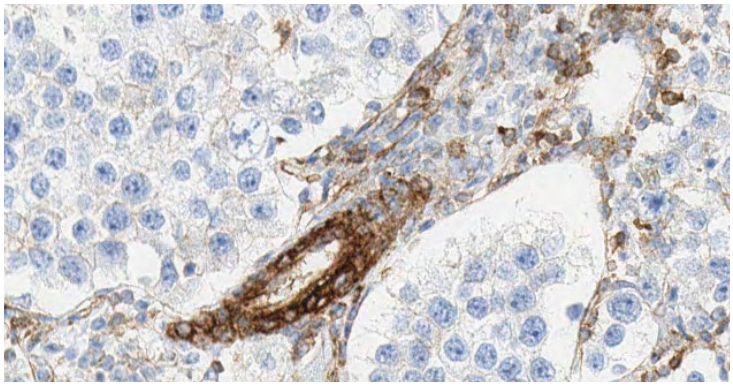

Head & neck cancer

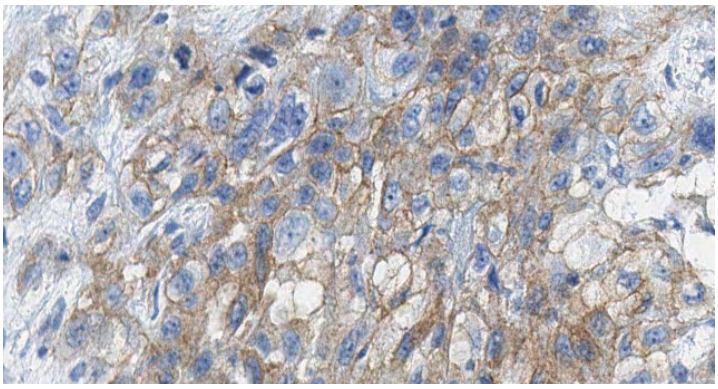

T cell lymphoma

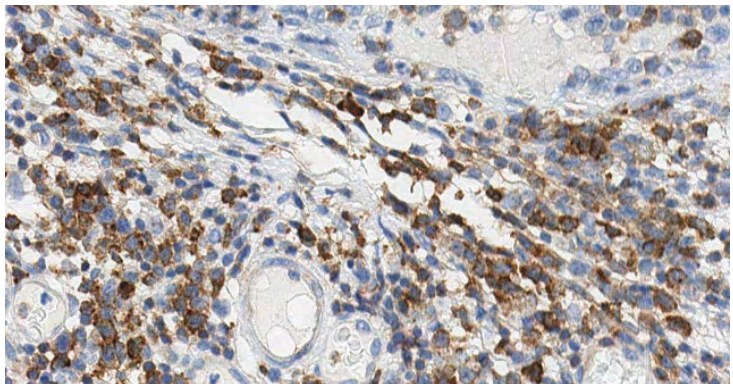

Invasive colon adenocarcinoma

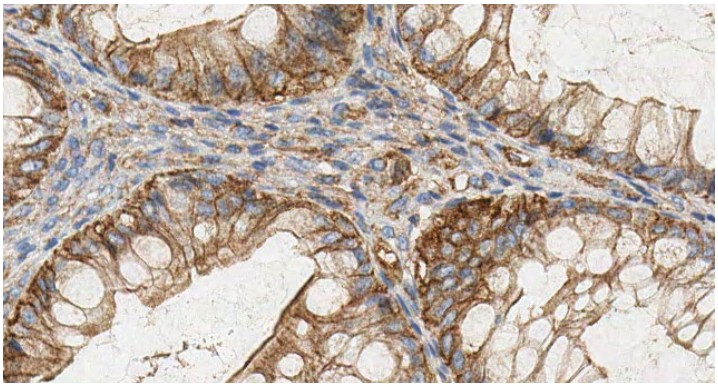

Invasive colon adenocarcinoma - Isotype control

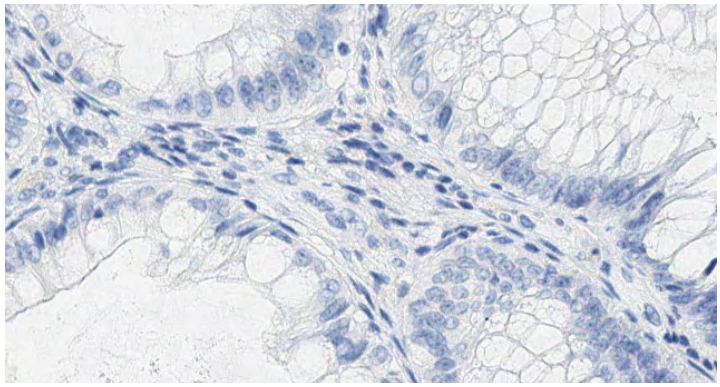

Figure 5. c-MET expression in cancer. IHC staining of multi-cancer human tissues using anti- c-Met (ab216574) or anti-rabbit IgG-isotype control antibody (ab172730). Positive staining in brown; nuclear hematoxylin counterstain in blue. Slides were scanned at 20x on Aperio® AT2 and imaged at 20x on Aperio® ImageScope.

c-MET expression in cancer (DISCOVERY ULTRA)

c-MET expression varied in the analysed cancer TMAs, with cervical cancer showing the highest H-score and breast cancer the lowest (a). The staining intensity of cohorts of cancer subtypes was also evaluated separately in scatter plots (with SD) (b-d).

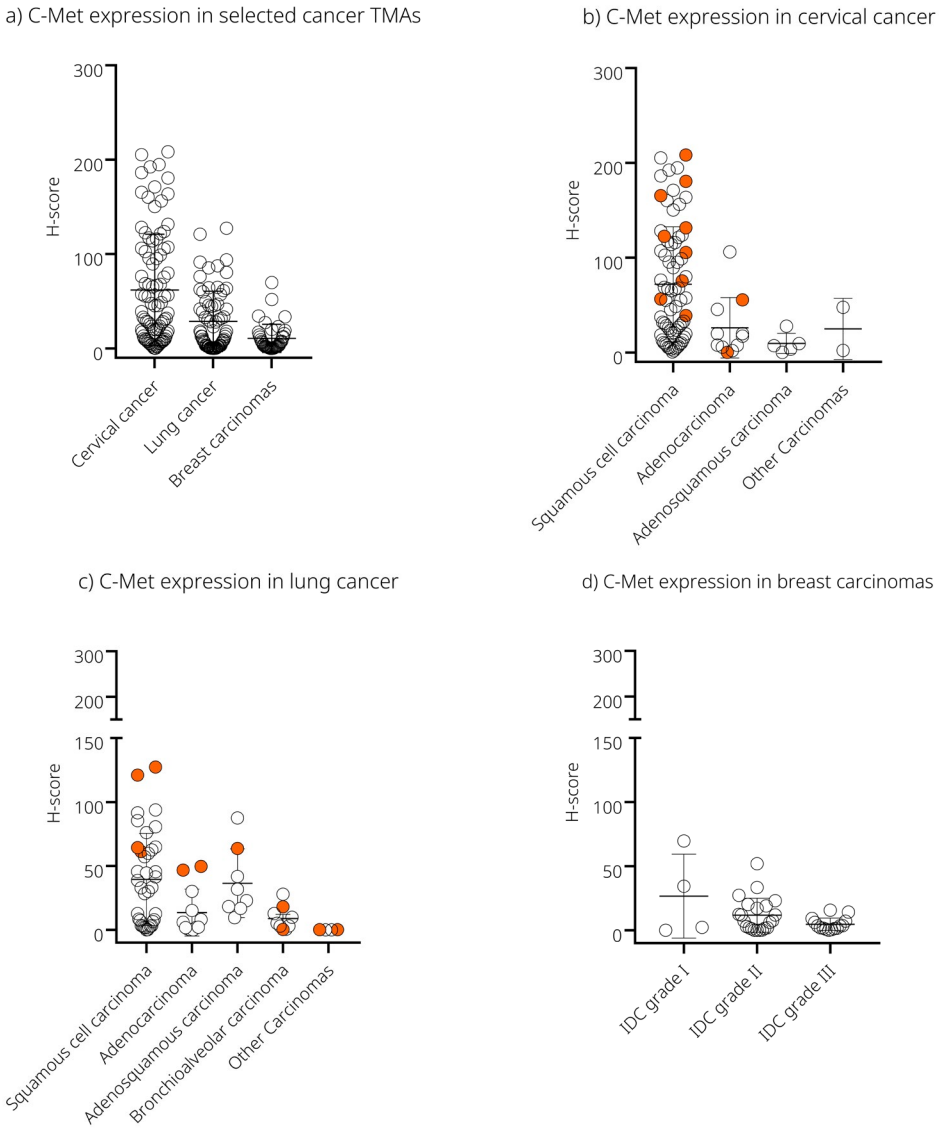

Figure 6. c-MET protein expression in a selection of cancer TMAs.
(a) The scatter plot (with SD) summarizes the relative average DAB intensity of C-MET expression in selected cancer TMA cores (cervical cancer (91), lung cancer (70) and breast cancer (41))
(b) H-score from 91 TMA cores/cases of cervical cancer (Squamous cell carcinoma (73), Adenocarcinoma (11), Adenosquamous carcinoma (5) and other carcinoma (Mucinous and endometrioid adenocarcinoma (2)). The IHC images corresponding to orange data points are shown in Figure 7.
(c) H-score from 70 TMA cores/cases of lung cancer (Squamous cell carcinoma (37), Adenocarcinoma (12), Adenosquamous carcinoma (8), Bronchioalveolar carcinoma (9) and other carcinoma (4) (Papillary adenocarcinoma (1) and Small cell carcinoma (3)). The IHC images corresponding to orange data points are shown in Figure 8.
(d) H-score averaged from 41 cases in duplicates (82 TMA cores) of breast cancer (grade I (1 & 1.5) (4), grade II (2 &2.5) (22) and grade III (15)).

c-MET expression in cervical cancer TMA (DISCOVERY ULTRA)

Below are the representative images of human cervical cancer TMA showing weak to strong c-MET expression.

c-MET

Normal cervix

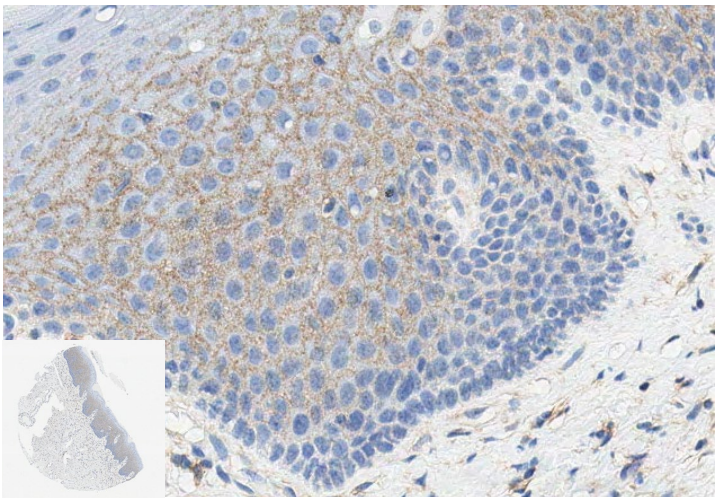

Cervical adenocarcinoma, Grade II (0.15)

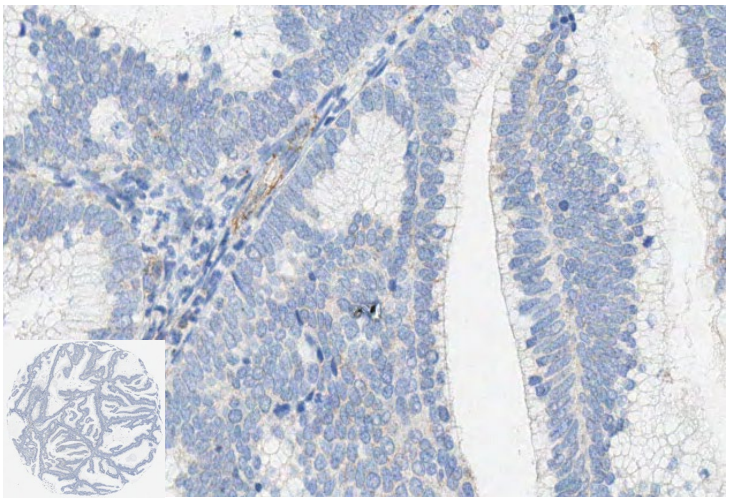

Cervical adenocarcinoma, Grade II-III (55.59)

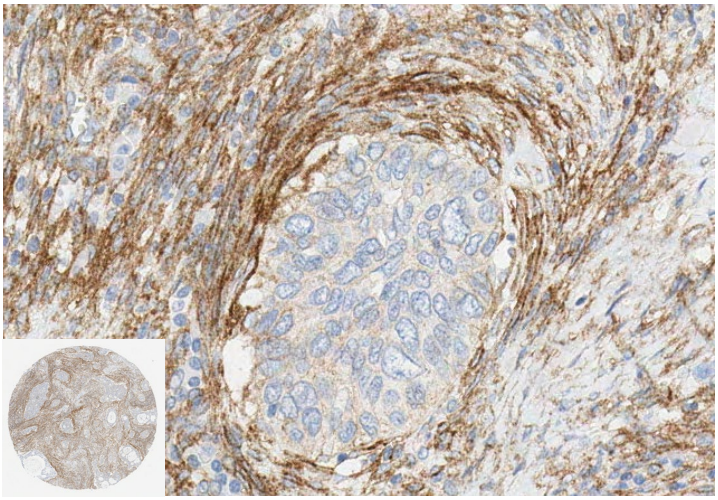

Squamous cell carcinoma, Grade I (38.88)

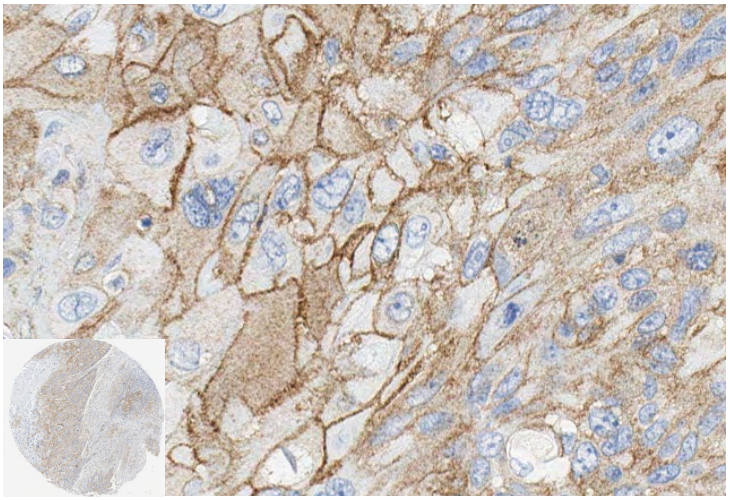

c-MET

Squamous cell carcinoma, Grade II (56.35)

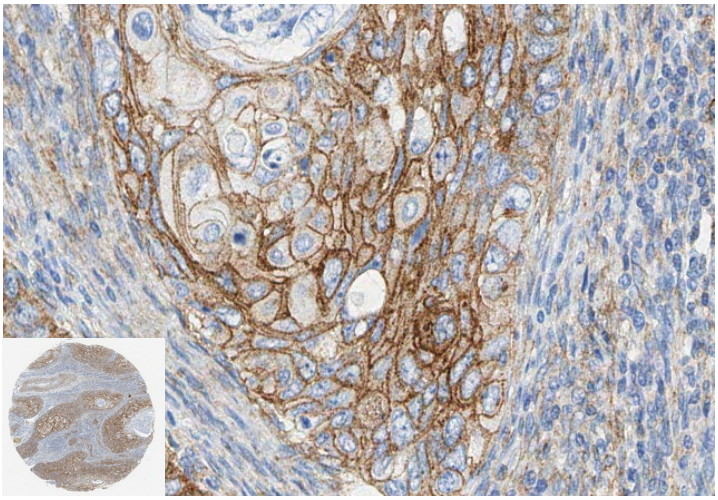

Squamous cell carcinoma, Grade I (0.0)

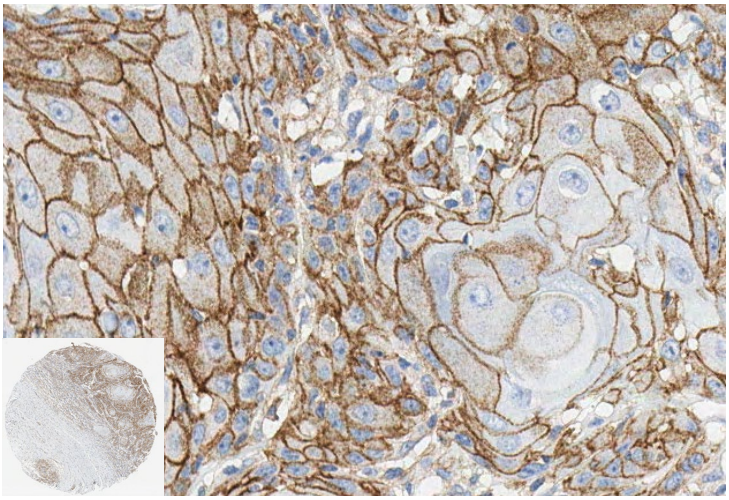

Squamous cell carcinoma, Grade I-II (105.5)

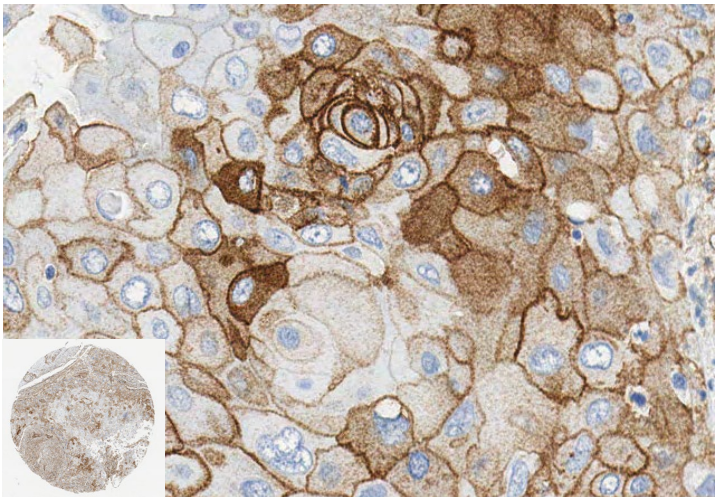

Squamous cell carcinoma, Grade II-III (122.53)

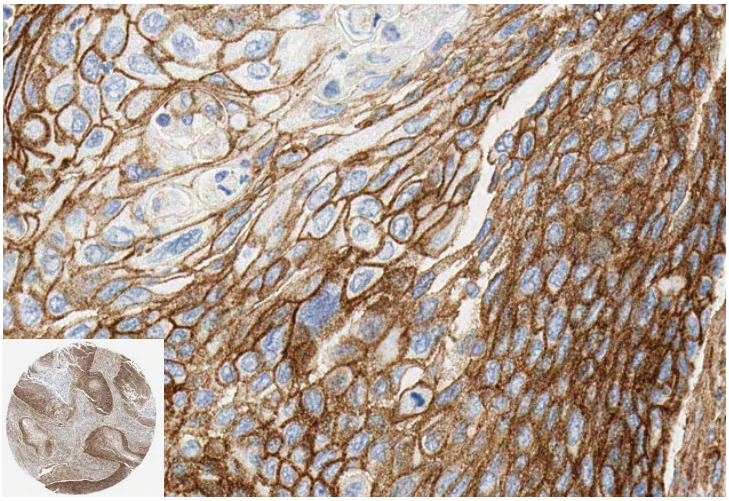

c-MET

Squamous cell carcinoma, Grade III (131.43)

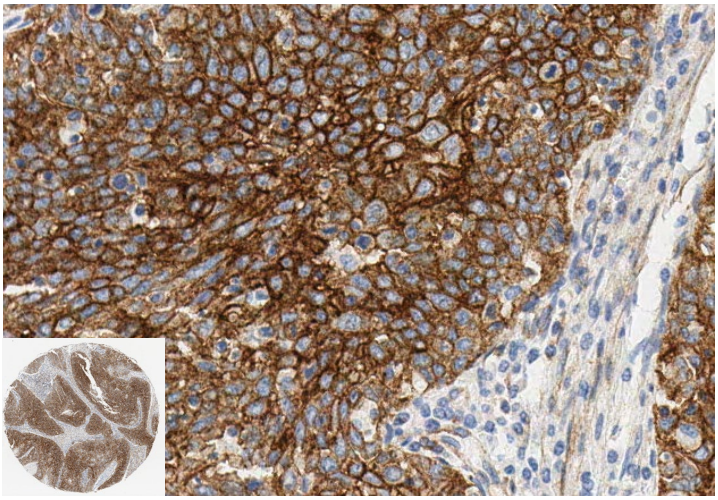

Squamous cell carcinoma, Grade III (165.41)

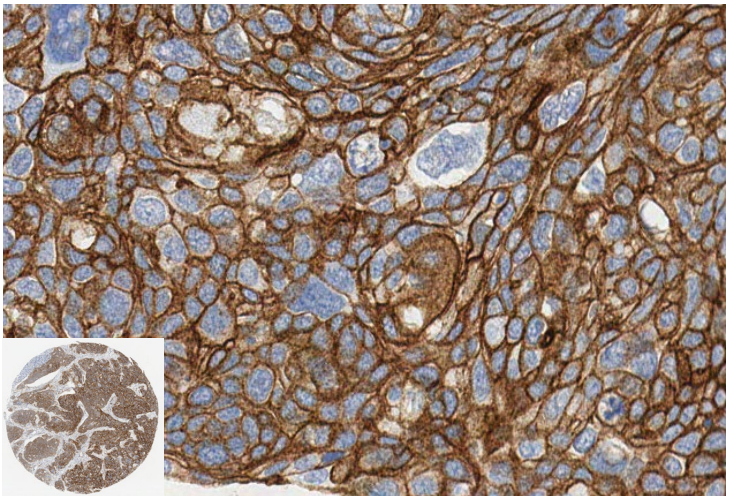

Squamous cell carcinoma, Grade III (180.48)

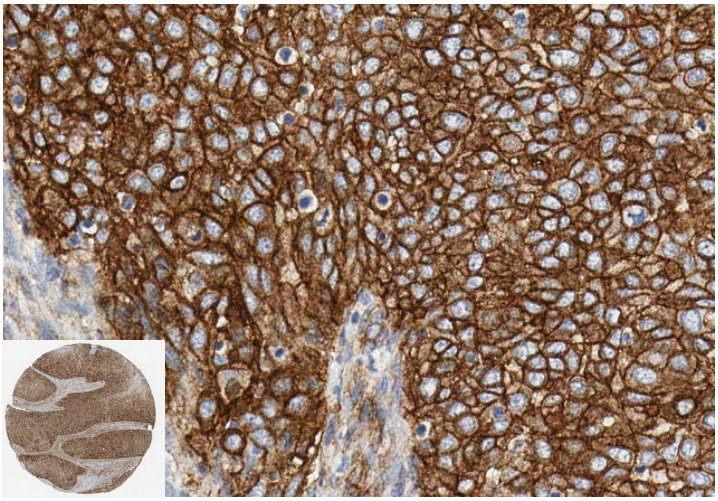

Squamous cell carcinoma, Grade III (208.32)

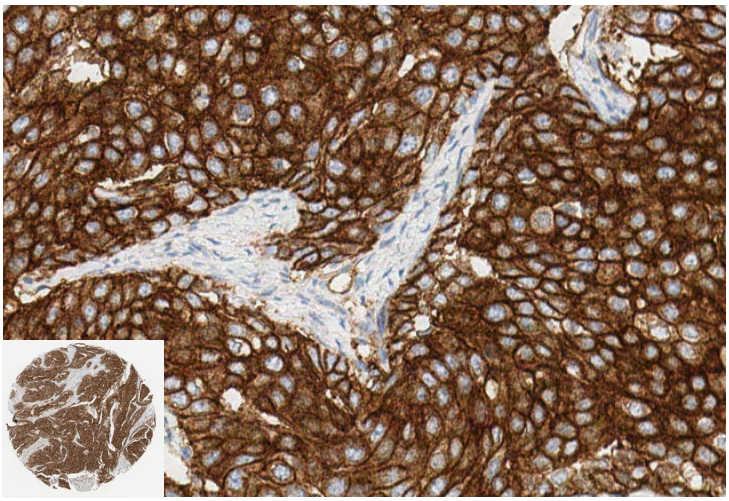

Figure 7. c-MET expression in cervical cancer. IHC images show weak, moderate or strong in brown (a-l); nuclear hematoxylin counterstain in blue. Slides were scanned at 20x (whole core insets at 5x) on Aperio® AT2 and imaged at 20x on Aperio® ImageScope.

c-MET expression in lung cancer TMA (DISCOVERY ULTRA)

Below are the representative images of human lung cancer TMA showing weak to strong c-MET expression.

c-MET

Papillary adenocarcinoma (0.25)

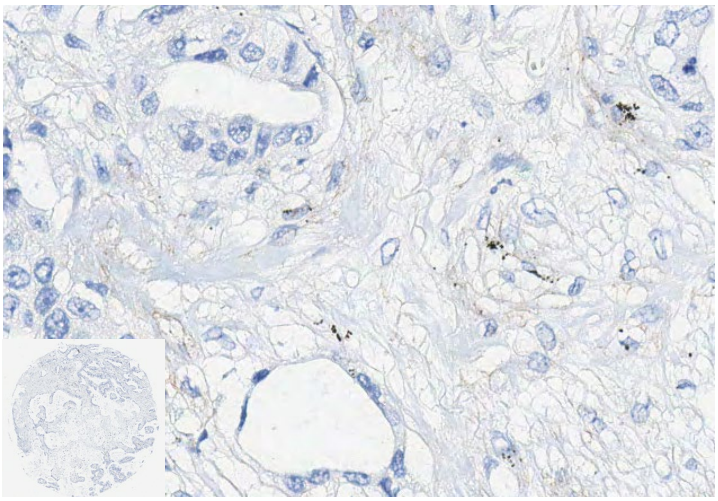

Small cell carcinoma (0.25)

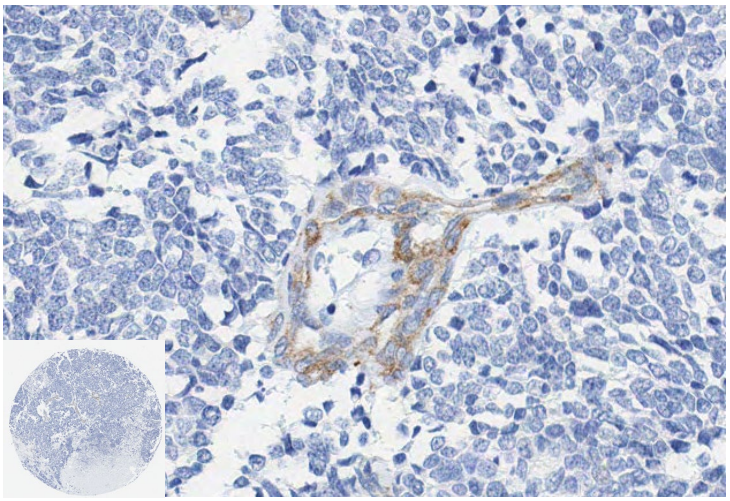

Bronchioloalveolar carcinoma (0.39)

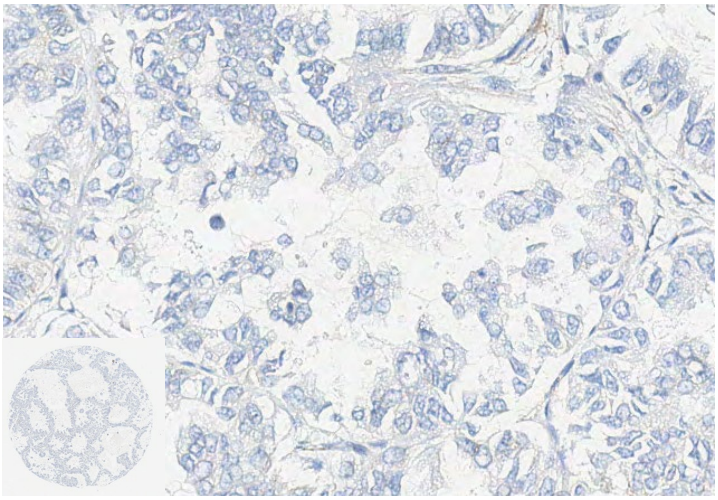

Bronchioloalveolar carcinoma (18.14)

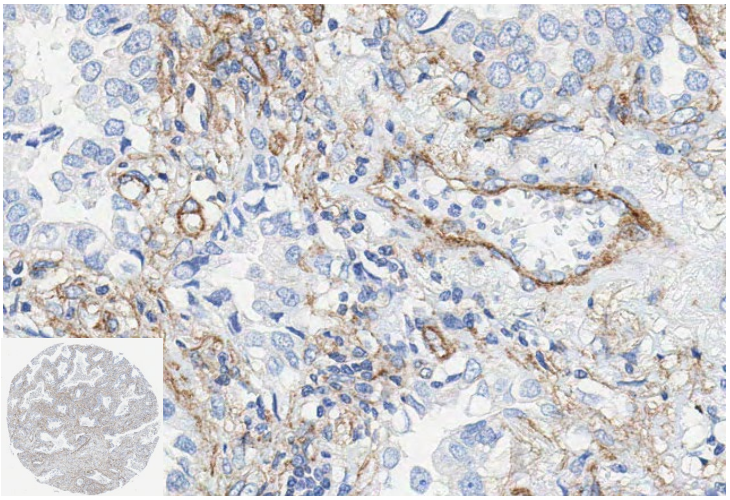

c-MET

Adenocarcinoma (46.79)

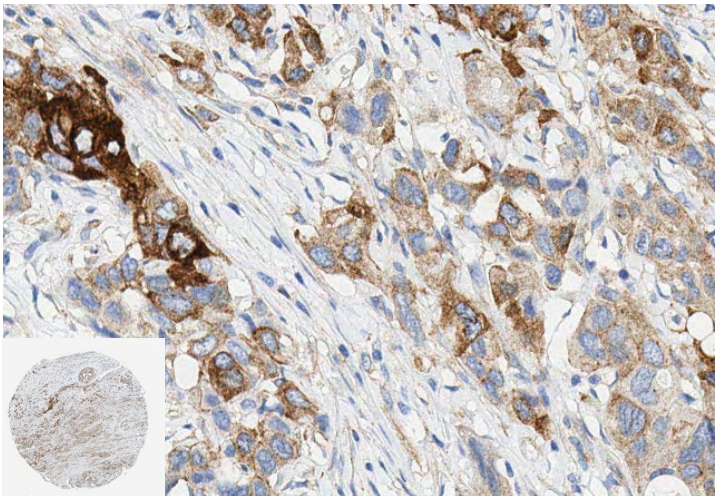

Adenocarcinoma (49.75)

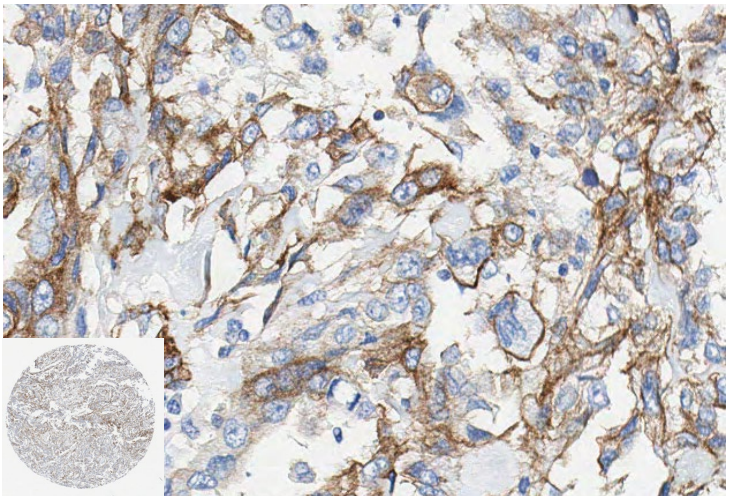

Adenosquamous carcinoma (63.66)

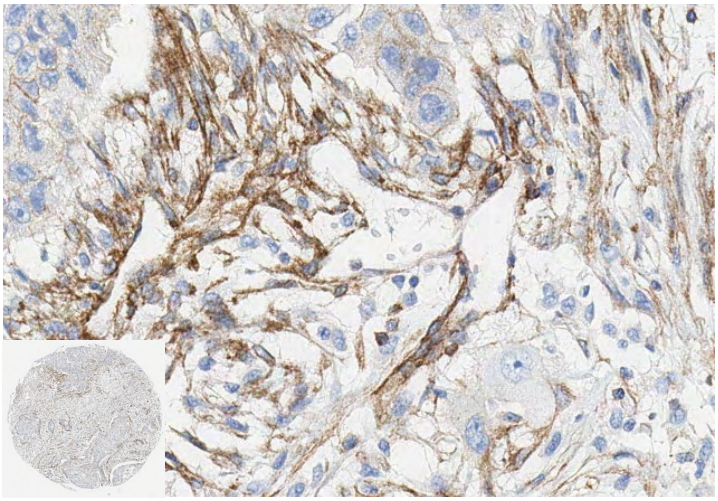

Adenosquamous carcinoma (87.62)

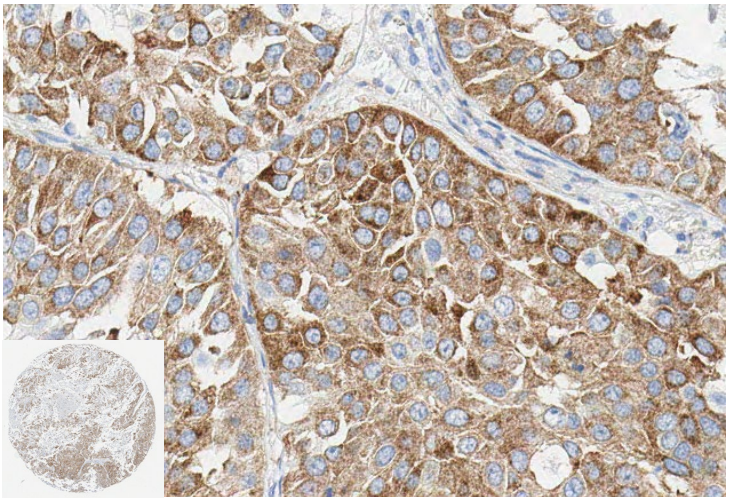

c-MET

Squamous cell carcinoma (61.66)

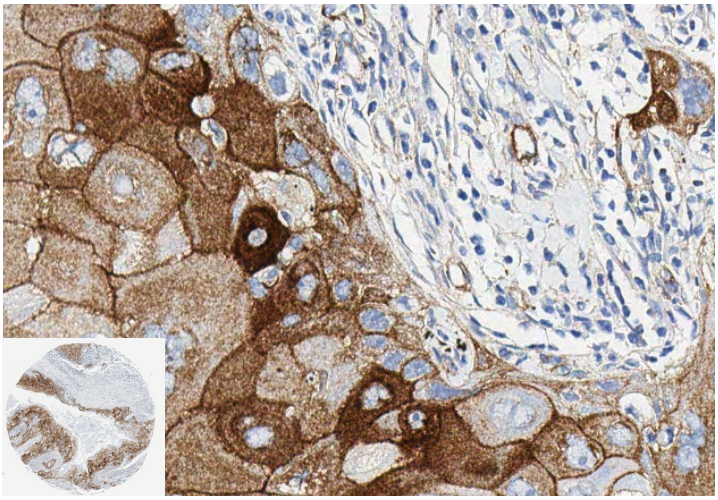

Squamous cell carcinoma (64.37)

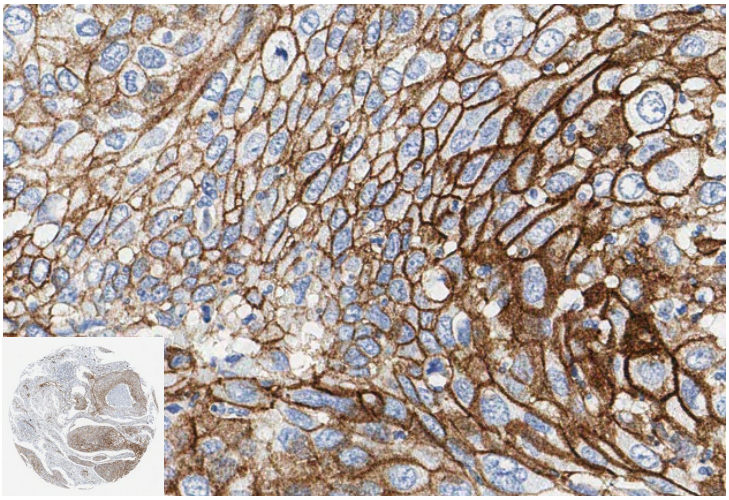

Squamous cell carcinoma (121.08)

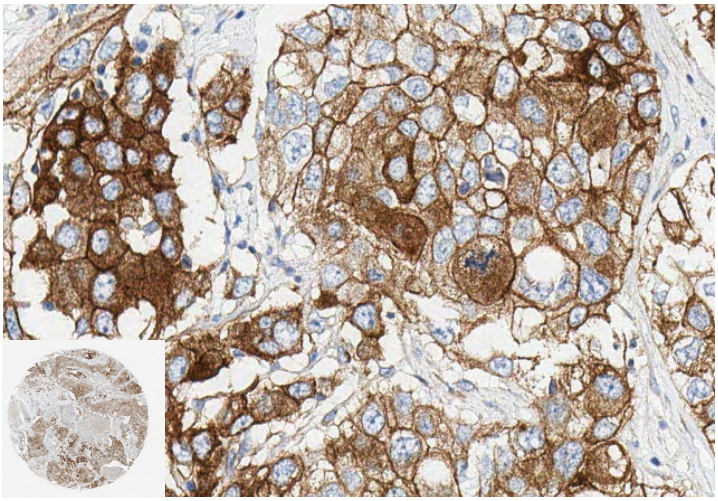

Squamous cell carcinoma (127.04)

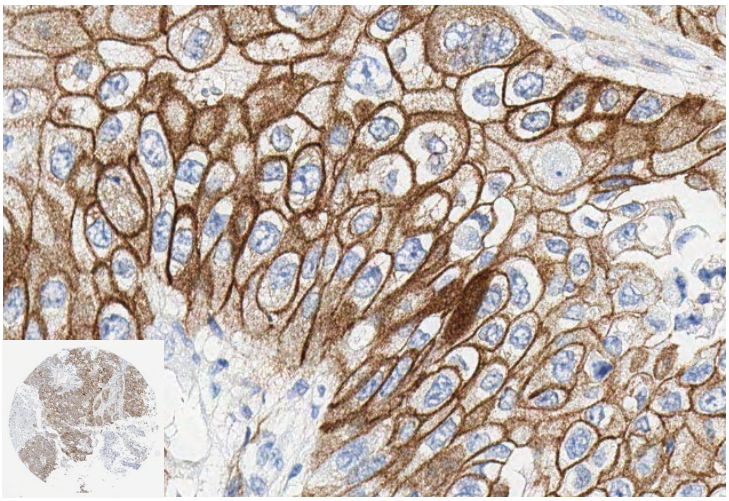

Figure 8: c-MET expression in lung cancer. IHC images show weak, moderate or strong in brown (a-l); nuclear hematoxylin counterstain in blue. Slides were scanned at 20x (whole core insets at 5x) on Aperio® AT2 and imaged at 20x on Aperio® ImageScope.

c-MET expression in breast cancer TMA (DISCOVERY ULTRA)

Below are the representative images of human breast cancer TMA showing weak to strong c-MET expression.

c-MET

IDC, Grade I (0.11)

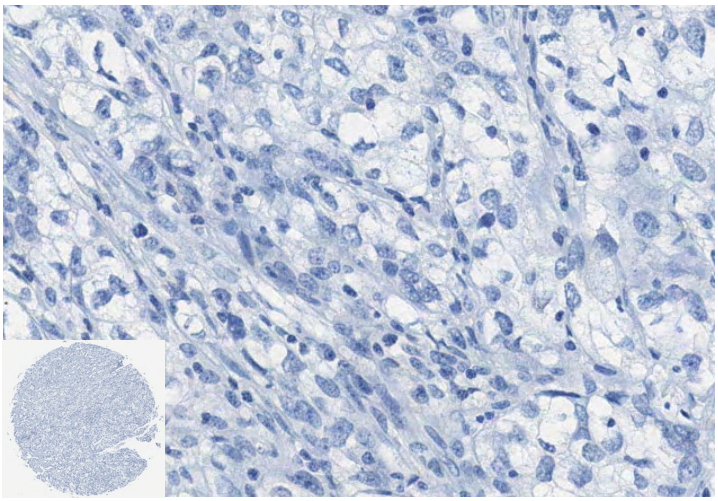

IDC, Grade II (4.65)

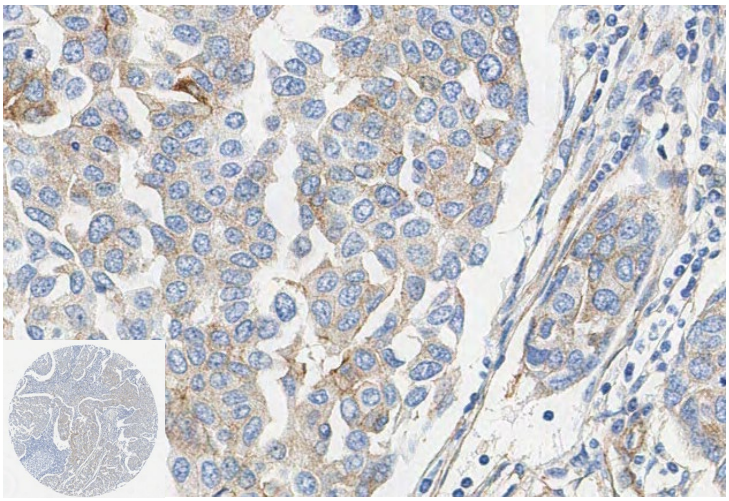

IDC, Grade III (9.14)

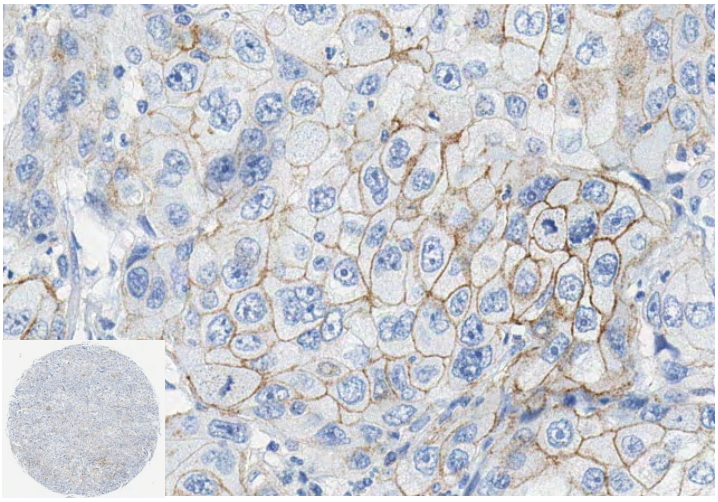

IDC, Grade III (9.62)

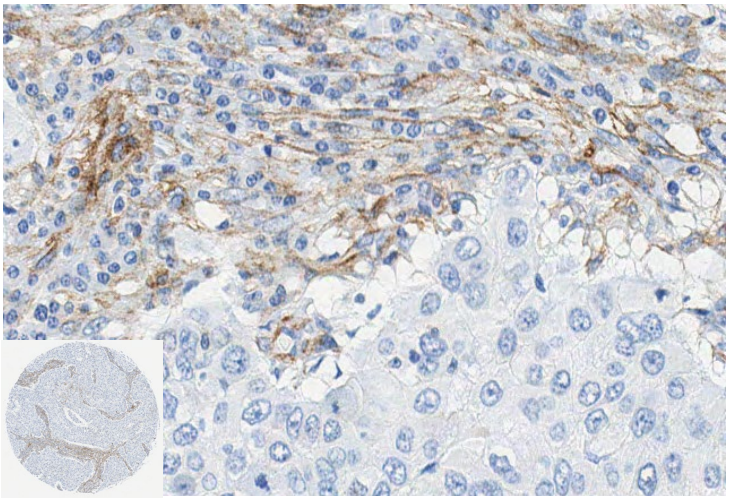

c-MET

IDC, Grade III (10.22)

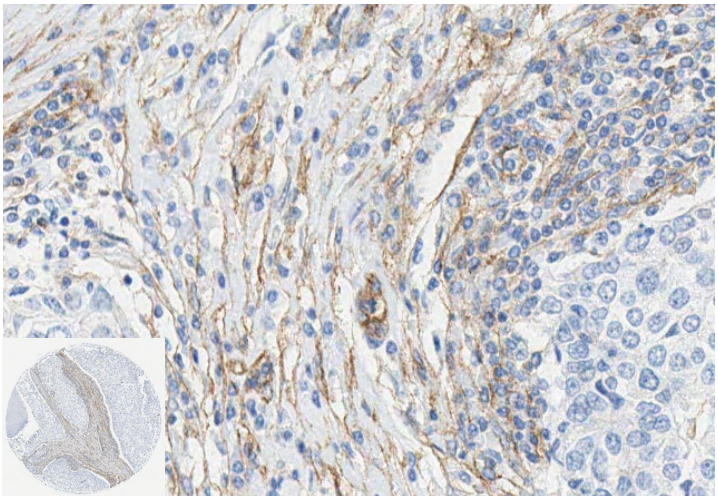

IDC, Grade II (13.98)

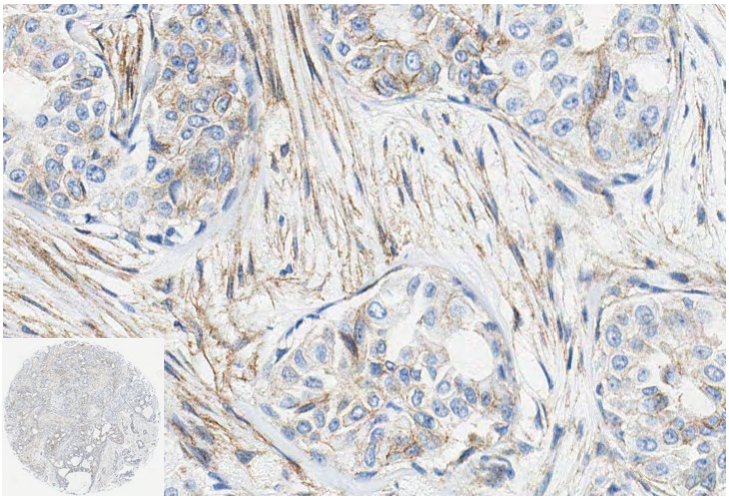

IDC, Grade II (22.06)

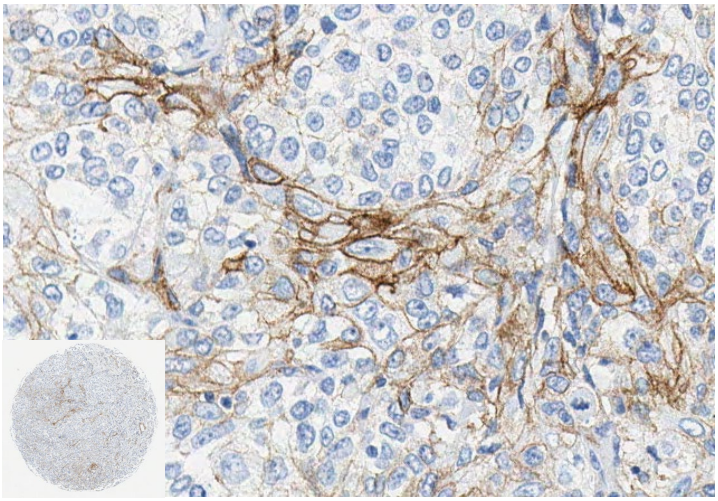

IDC, Grade II (29.85)

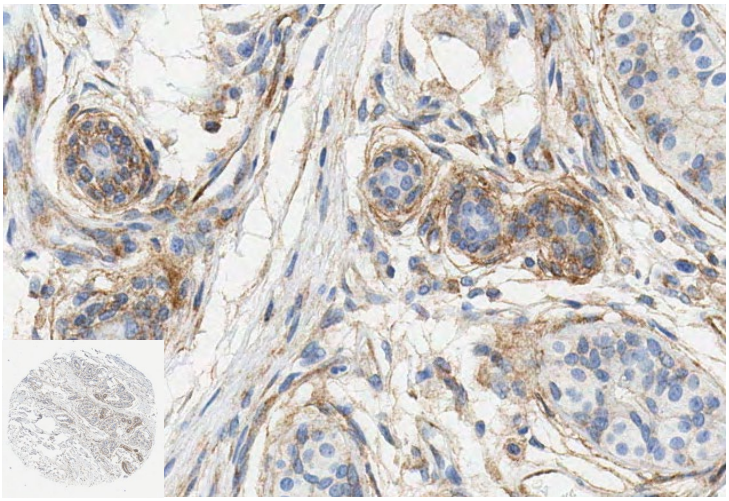

c-MET

IDC, Grade II (44.25)

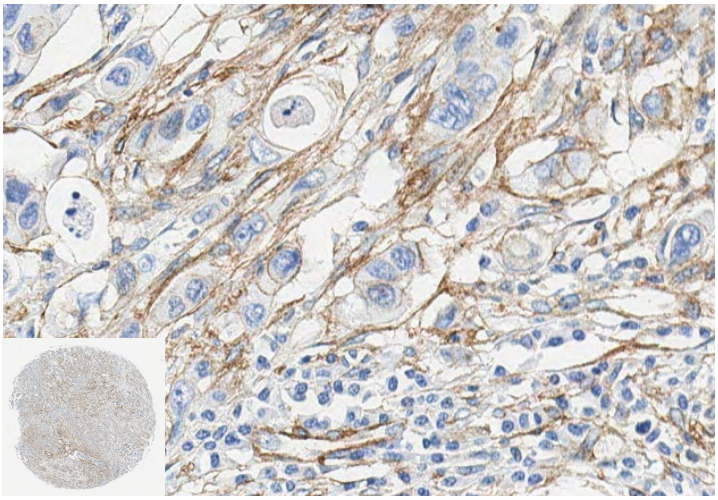

IDC, Grade II (59.41)

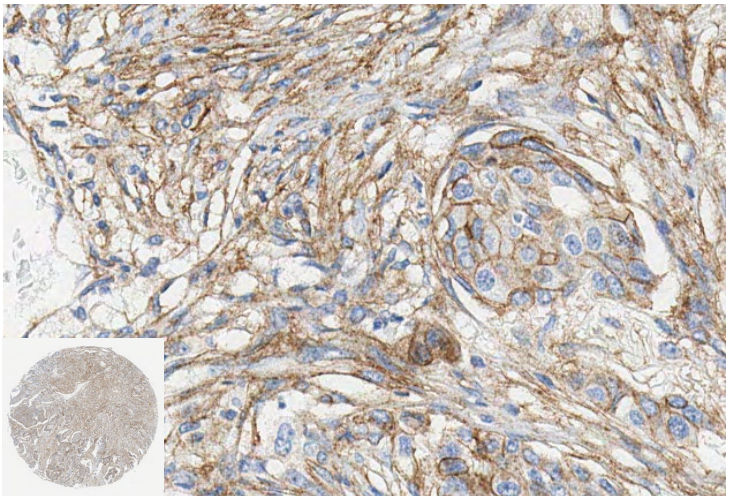

IDC, Grade I (69.75)

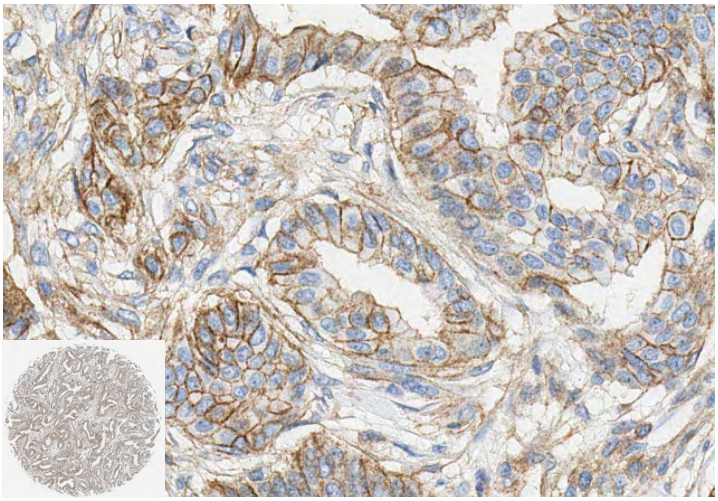

IDC, Grade II (67.70)

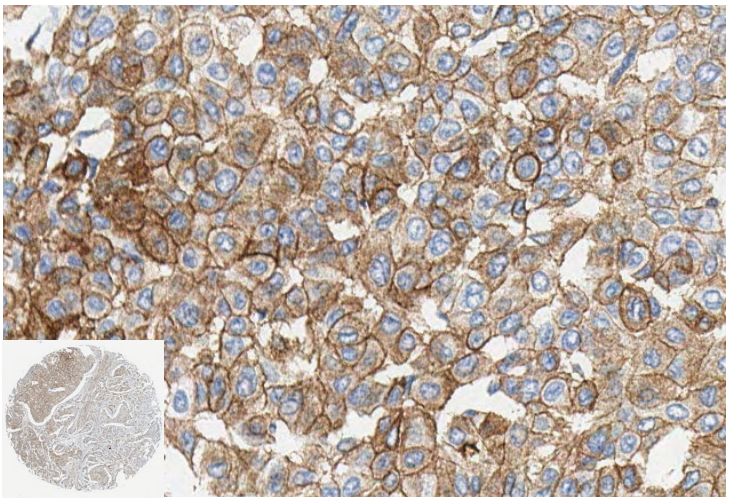

Figure 9: c-MET expression in breast cancer. IHC images show weak, moderate or strong in brown (a-l); nuclear hematoxylin counterstain in blue. Slides were scanned at 20x (whole core insets at 5x) on Aperio® AT2 and imaged at 20x on Aperio® ImageScope.

References

1. Goyal L, Muzumdar MD, Zhu AX. Targeting the HGF/c-MET pathway in hepatocellular carcinoma. Clin Cancer Res. 2013;19:2310–8.

2. Tavian D, De Petro G, Benetti A, Portolani N, Giulini SM, Barlati S. u-PA and c-MET mRNA expression is co-ordinately enhanced while hepatocyte growth factor mRNA is down-regulated in human hepatocellular carcinoma. Int J Cancer. 2000;87:644–9.

3. Taulli R, Scuoppo C, Bersani F, Accornero P, Forni PE, Miretti S, et al. Validation of met as a therapeutic target in alveolar and embryonal rhabdomyosarcoma. Cancer Res. 2006;66:4742–9

4. Yao JF, Li XJ, Yan LK, He S, Zheng JB, Wang XR, et al. Role of HGF/c-Met in the treatment of colorectal cancer with liver metastasis. J Biochem Mol Toxicol. 2019;33:e22316.

5. Du F, Li X, Feng W, Qiao C, Chen J, Jiang M, et al. SOX13 promotes colorectal cancer metastasis by transactivating SNAI2 and c-MET. Oncogene. 2020;39:3522–40.

6. Michikoshi H, Nakamura T, Sakai K, Suzuki Y, Adachi E, Matsugo S, et al. α-Lipoic acid-induced inhibition of proliferation and met phosphorylation in human non-small cell lung cancer cells. Cancer Lett. 2013;335:472–8.

7. Lee SJ, Lee J, Park SH, Park JO, Lim HY, Kang WK, et al. c-MET overexpression in colorectal cancer: a poor prognostic factor for survival. Clin Colorectal Cancer. 2018;17:165–9. .

8. Catenacci DV, Ang A, Liao WL, Shen J, O'Day E, Loberg RD, et al. MET tyrosine kinase receptor expression and amplification as prognostic biomarkers of survival in gastroesophageal adenocarcinoma. Cancer. 2017;123:1061–70.

9. Fan G, Zhang S, Gao Y, Greer PA, Tonks NK. HGF-independent regulation of MET and GAB1 by nonreceptor tyrosine kinase FER potentiates metastasis in ovarian cancer. Genes Dev. 2016;30:1542–57.

10. Zhang Y, Gao X, Zhu Y, Kadel D, Sun H, Chen J, et al. The dual blockade of MET and VEGFR2 signaling demonstrates pronounced inhibition on tumor growth and metastasis of hepatocellular carcinoma. J Exp Clin Cancer Res. 2018;37:93.

11. Du F, Li X, Feng W, Qiao C, Chen J, Jiang M, et al. SOX13 promotes colorectal cancer metastasis by transactivating SNAI2 and c-MET. Oncogene. 2020;39:3522–40.

12. Xing F, Liu Y, Wu SY, Wu K, Sharma S, Mo YY, et al. Loss of XIST in breast cancer activates MSN-c-Met and reprograms microglia via exosomal miRNA to promote brain metastasis. Cancer Res. 2018;78:4316–30.

13. Zambelli A, Biamonti G, Amato A. HGF/c-Met signalling in the tumor microenvironment. Adv Exp Med Biol. 2021;1270:31–44

14. Zhang Y, Nguyen TTT, Shang E, Mela A, Humala N, Mahajan A, et al. MET inhibition elicits PGC1α-dependent metabolic reprogramming in glioblastoma. Cancer Res. 2020;80:30–43.

15. Joo KM, Jin J, Kim E, Ho Kim K, Kim Y, Gu Kang B, et al. MET signaling regulates glioblastoma stem cells. Cancer Res. 2012;72:3828–38.

16. Rath P, Lal B, Ajala O, Li Y, Xia S, Kim J, et al. In vivo c-Met pathway inhibition depletes human glioma xenografts of tumor-propagating stem-like cells. Transl Oncol. 2013;6:104–11.

AB0407_v1.0_121824

17. Flores-Téllez TN, Villa-Treviño S, Piña-Vázquez C. Road to stemness in hepatocellular carcinoma. World J Gastroenterol. 2017;23:6750–76.

18. Huang WC, Tung SL, Chen YL, Chen PM, Chu PY. IFI44L is a novel tumor suppressor in human hepatocellular carcinoma affecting cancer stemness, metastasis, and drug resistance via regulating met/Src signaling pathway. BMC Cancer. 2018;18:609.

19. Jahangiri A, Nguyen A, Chandra A, Sidorov MK, Yagnik G, Rick J, et al. Cross-activating c-Met/β1 integrin complex drives metastasis and invasive resistance in cancer. Proc Natl Acad Sci USA. 2017;114:E8685–94.

20. Straussman R, Morikawa T, Shee K, Barzily-Rokni M, Qian ZR, Du J, et al. Tumour micro-environment elicits innate resistance to RAF inhibitors through HGF secretion. Nature. 2012;487:500–4.

21. Hugo W, Shi H, Sun L, Piva M, Song C, Kong X, et al. Non-genomic and immune evolution of melanoma acquiring MAPKi resistance. Cell. 2015;162:1271–85.

22. Bean J, Brennan C, Shih JY, Riely G, Viale A, Wang L, et al. MET amplification occurs with or without T790M mutations in EGFR mutant lung tumors with acquired resistance to gefitinib or erlotinib. Proc Natl Acad Sci USA. 2007;104:20932–7.

23. Jankowski K, Kucia M, Wysoczynski M, Reca R, Zhao D, Trzyna E, et al. Both hepatocyte growth factor (HGF) and stromal-derived factor-1 regulate the metastatic behavior of human rhabdomyosarcoma cells, but only HGF enhances their resistance to radiochemotherapy. Cancer Res. 2003;63:7926–35.

24. Huang WC, Tung SL, Chen YL, Chen PM, Chu PY. IFI44L is a novel tumor suppressor in human hepatocellular carcinoma affecting cancer stemness, metastasis, and drug resistance via regulating met/Src signaling pathway. BMC Cancer. 2018;18:609.

25. Jahangiri A, Nguyen A, Chandra A, Sidorov MK, Yagnik G, Rick J, et al. Cross-activating c-Met/β1 integrin complex drives metastasis and invasive resistance in cancer. Proc Natl Acad Sci USA. 2017;114:E8685–94.

26. Straussman R, Morikawa T, Shee K, Barzily-Rokni M, Qian ZR, Du J, et al. Tumour micro-environment elicits innate resistance to RAF inhibitors through HGF secretion. Nature. 2012;487:500–4.

27. Hugo W, Shi H, Sun L, Piva M, Song C, Kong X, et al. Non-genomic and immune evolution of melanoma acquiring MAPKi resistance. Cell. 2015;162:1271–85.

28. Bean J, Brennan C, Shih JY, Riely G, Viale A, Wang L, et al. MET amplification occurs with or without T790M mutations in EGFR mutant lung tumors with acquired resistance to gefitinib or erlotinib. Proc Natl Acad Sci USA. 2007;104:20932–7.

29. Jankowski K, Kucia M, Wysoczynski M, Reca R, Zhao D, Trzyna E, et al. Both hepatocyte growth factor (HGF) and stromal-derived factor-1 regulate the metastatic behavior of human rhabdomyosarcoma cells, but only HGF enhances their resistance to radiochemotherapy. Cancer Res. 2003;63:7926–35.

30. Natali PG, Prat M, Nicotra MR, et al. Overexpression of the met/HGF receptor in renal cell carcinomas. Int J Cancer 1996; 69: 212–7.

31. Olivero M, Rizzo M, Madeddu R, et al. Overexpression and activation of hepatocyte growth factor/scatter factor in human non-small-cell lung carcinomas. Br J Cancer 1996; 74: 1862–8.

32. Hellman A, Zlotorynski E, Scherer SW, et al. A role for common fragile site induction in amplification of human oncogenes. Cancer Cell 2002; 1: 89–97.

33. Di Renzo MF, Olivero M, Katsaros D, et al. Overexpression of the Met/HGF receptor in ovarian cancer. Int J Cancer 1994; 58: 658–62.

34. Maulik G, Kijima T, Ma PC, et al. Modulation of the c-Met/hepatocyte growth factor pathway in small cell lung cancer. Clin Cancer Res 2002; 8: 620–7.

35. Cerami E, Gao J, Dogrusoz U, Gross BE, Sumer SO, Aksoy BA, Jacobsen A, Byrne CJ, Heuer ML, Larsson E, Antipin Y, Reva B, Goldberg AP, Sander C, Schultz N. The cBio cancer genomics portal: an open platform for exploring multidimensional cancer genomics data. Cancer Discov. 2012 May;2(5):401-4. doi: 10.1158/2159-8290.CD-12-0095. Erratum in: Cancer Discov. 2012 Oct;2(10):960. PMID: 22588877; PMCID: PMC3956037.

36. Gao J, Aksoy BA, Dogrusoz U, Dresdner G, Gross B, Sumer SO, Sun Y, Jacobsen A, Sinha R, Larsson E, Cerami E, Sander C, Schultz N. Integrative analysis of complex cancer genomics and clinical profiles using the cBioPortal. Sci Signal. 2013 Apr 2;6(269):pl1. doi: 10.1126/scisignal.2004088. PMID: 23550210; PMCID: PMC4160307.

37. de Bruijn I, Kundra R, Mastrogiacomo B, Tran TN, Sikina L, Mazor T, Li X, Ochoa A, Zhao G, Lai B, Abeshouse A, Baiceanu D, Ciftci E, Dogrusoz U, Dufilie A, Erkoc Z, Garcia Lara E, Fu Z, Gross B, Haynes C, Heath A, Higgins D, Jagannathan P, Kalletla K, Kumari P, Lindsay J, Lisman A, Leenknegt B, Lukasse P, Madela D, Madupuri R, van Nierop P, Plantalech O, Quach J, Resnick AC, Rodenburg SYA, Satravada BA, Schaeffer F, Sheridan R, Singh J, Sirohi R, Sumer SO, van Hagen S, Wang A, Wilson M, Zhang H, Zhu K, Rusk N, Brown S, Lavery JA, Panageas KS, Rudolph JE, LeNoue-Newton ML, Warner JL, Guo X, Hunter-Zinck H, Yu TV, Pilai S, Nichols C, Gardos SM, Philip J; AACR Project GENIE BPC Core Team, AACR Project GENIE Consortium; Kehl KL, Riely GJ, Schrag D, Lee J, Fiandalo MV, Sweeney SM, Pugh TJ, Sander C, Cerami E, Gao J, Schultz N. Analysis and Visualization of Longitudinal Genomic and Clinical Data from the AACR Project GENIE Biopharma Collaborative in cBioPortal. Cancer Res. 2023 Dec 1;83(23):3861-3867. doi: 10.1158/0008-5472.CAN-23-0816. PMID: 37668528; PMCID: PMC10690089.

38. Blum A, Wang P, Zenklusen JC. SnapShot: TCGA-Analyzed Tumors. Cell. 2018 Apr 5;173(2):530. doi: 10.1016/j.cell.2018.03.059. PMID: 29625059.

Let’s work together:
Connect with us at oncology@abcam.com

progress happens together
abcam

danaher